STUK-TR 10 / AUGUST 2011

TR

# Handling of hydrogeochemical relations in erosion and swelling pressure models for the buffer and backfill

Randolph Arthur

Säteilyturvakeskus
Strålsäkerhetscentralen
Radiation and Nuclear Safety Authority

STUK

STUK-TR 10 / AUGUST 2011

# Handling of hydrogeochemical relations in erosion and swelling pressure models for the buffer and backfill

Part I: A review of surface-chemical concepts used in models of buffer erosion

Part II: An evaluation of swelling pressure models for the buffer and backfill

Randolph Arthur
INTERA, Inc

Responsible in STUK has been Ari Luukkonen

**STUK** • **SÄTEILYTURVAKESKUS**
**STRÅLSÄKERHETSCENTRALEN**
**RADIATION AND NUCLEAR SAFETY AUTHORITY**

Osoite/Address • Laippatie 4, 00880 Helsinki
Postiosoite / Postal address • PL / P.O.Box 14, FIN-00881 Helsinki, FINLAND
Puh./Tel. (09) 759 881, +358 9 759 881 • Fax (09) 759 88 500, +358 9 759 88 500 • www.stuk.fi

The conclusions presented in the STUK report series are those of the authors and do not necessarily represent the official position of STUK.

ISBN 978-952-478-638-6 (print, Edita Prima Oy, Finland 2011)
ISBN 978-952-478-639-3 (pdf)
ISSN 1796-7171

*ARTHUR Randolph. Handling of hydrogeochemical relations in erosion and swelling pressure models for the buffer and backfill. Part I: A review of surface-chemical concepts used in models of buffer erosion. Part II: An evaluation of swelling pressure models for the buffer and backfill. STUK-TR 10. Helsinki 2011. 4 pp + 30 pp + 15 pp.*

**Keywords:** nuclear waste, KBS-3 repository, bentonite buffer, tunnel backfill, chemical erosion, swelling pressure, modeling concepts

# Foreword

This documentation has been compiled from two separate reviews related to chemical concepts used in buffer-erosion models and swelling-pressure models for the buffer and backfill. Both reviews were ordered by STUK from Dr. Randolph Arthur, and were finished by him in September 2010 and July 2011, respectively. The reviews evaluate the state-of-the-art knowledge concerning both topics and are intended to assist STUK in its evaluation of confidence in the long-term performance of the buffer and backfill in the engineered barrier system of a nuclear waste repository. This background information will help STUK make a judgment as to what degree of confidence is needed for a successful construction license application, and what level of maturity in the knowledge of system performance will be required later when an operation license application is considered.

*ARTHUR Randolph. Hydrogeokemiallisten riippuvuuksien käsittely puskurin ja tunnelitäytteen eroosio- ja paisuntapainemalleissa. Osa I: Katsaus puskurieroosiomallien pintakemian kuvaukseen. Osa II: Arvio puskurin ja tunnelitäytteen paisuntapainemalleista. STUK-TR 10. Helsinki 2011. 4 s + 30 s + 15 s.*

**Avainsanat:** ydinjäte, KBS-3 loppusijoituslaitos, bentoniittipuskuri, tunnelitäyte, kemiallinen eroosio, paisuntapaine, mallinnusperusteet

# Esipuhe

Tämä dokumentaatio on koostettu kahdesta erillisestä kirjallisuuskatsauksesta, jotka liittyvät puskurieroosiomalleissa käytettyihin kemiallisiin käsitteistöihin sekä puskurin ja tunnelitäytteen paisumisen kuvaamiseen käytettyihin malleihin. Kummatkin katsaukset ovat STUKin Dr Randolph Arthur'lta tilaamia ja ne ovat valmistuneet syyskuussa 2010 (eroosio) ja heinäkuussa 2011 (paisuminen). Katsaukset arvioivat kansainvälistä tietämyksen tasoa sekä eroosion että paisumisen aihepiireistä. Niiden tarkoituksena on auttaa STUKia arvioimaan ydinjätteen loppusijoituslaitoksen teknisiin päästöesteisiin kuuluviin puskuriin ja tunnelitäytteeseen liitettyjä pitkäaikaisturvallisuuden perusteluja. Osin tuotettujen taustatietojen perusteella STUK tekee ratkaisunsa, mitkä ovat hyväksyttävän tasoiset perustelut eroosion ja paisumisen aihepiireistä rakentamislupahakemuksessa ja mikä tietämyksen taso loppusijoitussysteemin toimintakyvystä tullaan vaatimaan, kun loppusijoituslaitoksen käyttölupaa aikanaan harkitaan.

# Part I: A review of surface-chemical concepts used in models of buffer erosion

# Contents

SUMMARY I-3

1 INTRODUCTION I-4

2 TREATMENT OF BUFFER EROSION IN CONCEPTUAL MODELS AND SAFETY ASSESSMENTS I-5
2.1 Conceptual models I-5
2.2 Treatment of buffer erosion in SR-Can I-7

3 SURFACE-CHEMICAL CONCEPTS GOVERNING CLAY COLLOID FORMATION AND STABILITY I-9
3.1 Colloid terminology I-9
3.2 DLVO theory I-9
3.2.1 Electrical conditions at the clay-water interface I-10
3.2.2 Interaction energies among colloidal particles I-11
3.3 Effects of aqueous chemistry and temperature on colloid stability I-14

4 UNCERTAINTIES IN SURFACE-CHEMICAL CONCEPTS APPLIED TO MODELS OF BUFFER EROSION I-16
4.1 Deficiencies in DLVO theory applied to clay colloids I-16
4.2 Effects of clay composition on stability relations among sols, gels and flocs I-17

5 SUPPLEMENTARY EROSION CONSIDERATIONS I-19
5.1 Recent developments in modeling buffer erosion I-19
5.2 Potential impacts of buffer erosion on safety functions and performance targets I-20
5.3 Possible issues in dealing with buffer erosion in a safety case I-22
5.3.1 Mass-loss tolerances I-22
5.3.2 Uncertainties in buffer erosion models I-22
5.3.3 Geochemical constraints on sol stability I-22
5.3.4 Uncertainties in the characteristics of glacial meltwaters I-23
5.4 Relative safety significance of different types of buffer erosion I-23
5.5 Possible engineering measures to prevent buffer erosion I-23

6 CONCLUDING REMARKS I-25

7 REFERENCES I-27

# Summary

This report reviews surface-chemical concepts governing the formation and stability of clay colloids, and considers how these concepts might be used in models of buffer (chemical) erosion in a KBS-3 repository for spent nuclear fuel. There is a consensus among surface chemists that although theoretical treatments of clay colloid behavior are generally correct, they also suffer from important deficiencies. The deficiencies result from an oversimplification of the properties of real colloids, and from a failure to consider forces acting to stabilize or flocculate colloidal systems under certain environmental conditions, and at small inter-particle separation distances such as will exist in highly compacted buffer materials. It is unclear whether sufficient progress can be made over the next few years to adequately resolve these limitations. If not, dealing with the issue of buffer erosion in a safety-assessment context may require consideration of other features, events and processes (FEPs) that could also play an important role in the erosion process. It is recommended that STUK should consider carrying out critical evaluations of such FEPs in order to further prepare for its review of future license applications for a spent-fuel repository at Olkiluoto.

# 1 Introduction

Chemical erosion of the bentonite buffer in a KBS-3 repository for spent nuclear fuel refers to a process in which the constituent clay minerals are suspended as colloids and transported away from deposition holes in flowing groundwater. Chemical erosion differs from physical erosion, which involves the release of bentonite particles at the buffer-groundwater interface by shear forces acting on the particles by flowing groundwater, or, in the process of "piping", by hydraulic forces acting on the buffer during saturation (Börgesson and Sandén, 2006; Liu and Neretnieks, 2006; Jussila 2007). Physical erosion is not considered further here.

Colloid formation at the bentonite-groundwater interface is possible in repository scenarios calling for the transient migration of glacial meltwaters to repository depths. This is because stable suspensions of clay colloids tend to form in contact with aqueous solutions that are relatively dilute (*e.g.*, Miller and Marcos, 2007; Missana *et al.*, 2003). Under such conditions, erosion of as little as 1200 kg of bentonite from a deposition hole (about 6% of the initial dry mass) could generate advective-transport conditions in the buffer (Börgesson and Hernelind, 2006). This is a potential concern because advection would enhance the transport rate of corrodants to the canister's surface, thus increasing corrosion rates. The recent SR-Can safety assessment, for example, estimates that buffer erosion could lead to the failure of some tens of canisters at the Forsmark site over an assessment time frame of one million years if pessimistic hydraulic conditions are assumed, together with cautious assumptions regarding sulfide concentrations and deposition hole acceptance criteria (SKB 2006). Calculated risks are below the regulatory risk limit during the first 100,000 years of repository evolution, however.

Both Posiva and SKB are currently developing approaches for dealing with the potential impacts of buffer erosion in a safety-assessment context. Experiments and modeling related to chemical erosion are planned in Posiva's BENTO program (Posiva 2006). SKB have established a multi-year R&D program devoted to this topic, and results obtained over the past several years are available at *www.kemi.kth.se/nuchem/be*. SKB is currently in the process of defining an approach that will be used to deal with the issue of buffer erosion in the upcoming SR-Site performance assessment.

It is likely that the approaches noted above will rely to some extent on conceptual and numerical models of buffer erosion that are constrained by fundamental surface-chemical concepts governing the formation and stability of clay colloids. The present report reviews these concepts and attempts to assess how associated uncertainties could impact the reliability of predictions made using buffer erosion models. The effects of these uncertainties on assessments of repository performance are a key concern that STUK will have to consider in future reviews of license applications from Posiva for a spent-fuel repository in Finland.

The report is organized as follows. Section 2 describes how buffer erosion has been handled previously in conceptual models and safety assessments. Surface-chemical concepts that have been developed to explain the formation and stability of clay colloids are then reviewed in Section 3. Section 4 addresses limitations in these concepts and associated potential impacts on models of buffer erosion. Section 5 summarizes some supplementary views on recently developed models of buffer erosion. Section 6 considers a broader perspective on features, events and processes related to buffer chemical erosion that could provide a framework for STUK, possibly in collaboration with SSM, to further evaluate the treatment of this issue in future safety cases that will be put forward by Posiva (and SKB).

# 2 Treatment of buffer erosion in conceptual models and safety assessments

*Conceptual models of buffer chemical erosion have been developed mainly by SKB (SKB 2004; Liu and Neretnieks 2006) and are described below. An approach used by SKB to deal with this issue in the SR-Can safety assessment is also discussed. Posiva has not yet formally considered buffer erosion in a safety assessment of a KBS-3 repository at Olkiluoto.*

## 2.1 Conceptual models

SKB's prototype conceptual model of buffer erosion is described in the SR-Can Interim Process Report (SKB 2004; Appendix A). A schematic overview of the model is shown in Figure 1, where it can be seen that bentonite is assumed to penetrate a fracture that intersects a deposition hole. The penetration distance is controlled at steady state by the swelling pressure and by frictional forces acting at the interface between the extruded bentonite and fracture surface. Börgesson and Nilsson (2008) divide the extruded portion of the bentonite within the fracture into four domains having distinctly different rheological properties. From the deposition hole outward these domains include a solid mass of bentonite (zone A), a gel zone (zone B), and two sol zones, including a semi-fluid zone (zone C1) and a fluid zone (zone C2).[1] Zones B, C1 and C2 do not exist if the exchange sites on montmorillonite contain predominantly Ca. Moreno *et al*. (2008) note that bentonite could extrude about 4 m into a fracture if groundwater flow velocities are low (less than about 1 m $yr^{-1}$), and about 0.5 m into a fracture if groundwater velocities are high (greater than about 100 m $yr^{-1}$).

SKB adopts the concept of a critical coagulation concentration (CCC) for "free" (*i.e.*, uncomplexed) $Ca^{2+}$ to account for ionic-strength effects on colloid stability. This cation is selected because it is relatively abundant in groundwaters of the Fennoscandian Shield, and because its divalent character strongly influences colloid stability in accordance with the Schulze-Hardy rule (see Section 3.2). SKB assumes that the CCC for $Ca^{2+}$ is 1 mM. The bentonite within the fracture (Figure 1) is thus assumed to be stable if the concentration of $Ca^{2+}$ in the bentonite porewater is greater than this value. Conversely, colloidal suspensions of the

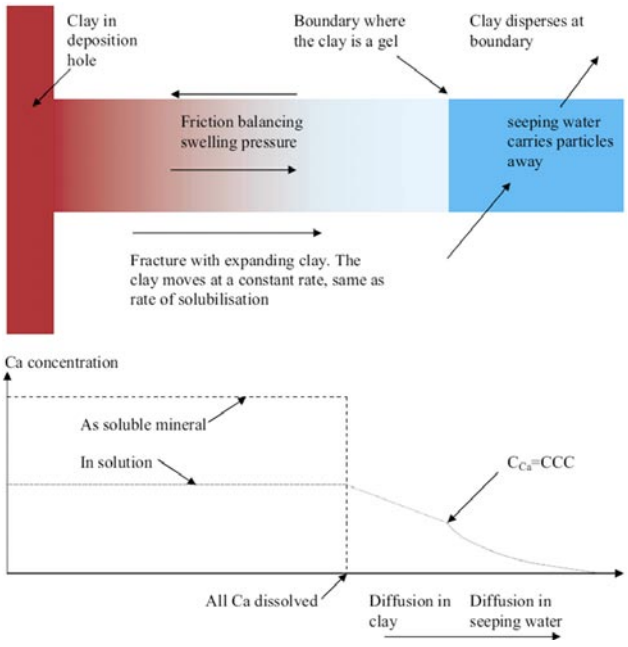


**Figure 1.** Conceptual model of buffer erosion (SKB 2004). The buffer extrudes a certain distance into the fracture under the control of swelling-pressure and frictional forces. The concentration of $Ca^{2+}$ in the seeping groundwater is assumed to be less than the CCC. The $Ca^{2+}$ concentration at the interface between the groundwater and buffer is equal to the CCC (i.e., because the gel is stable at that point). Calcium in the buffer's porewater diffuses toward the groundwater, and this is accompanied by dissolution of Ca-bearing minerals.

1 See Section 3.1 for notes regarding colloid terminology used in this report.

smectite clays form if $Ca^{2+}$ concentrations are below this value. Bentonite can persist at the bentonite-groundwater interface as long as the concentration of $Ca^{2+}$ in the groundwater is at or above the CCC.

SKB assumes that at some point in the future the extruded bentonite (Figure 1) comes into contact with groundwater having a $Ca^{2+}$ concentration below the CCC. A possible scenario compatible with this assumption involves the migration of dilute glacial meltwaters to repository depths at times when the repository is overlain by a warm-based ice sheet (SKB 2006). A mass balance is used to estimate the extent to which the buffer would be transformed into a stable colloidal suspension and carried away with the flowing groundwater. This results in the following equation (SKB 2004):

$$N_{clay} = \left( \frac{Q_{eq}(c_i - c_w)}{\varepsilon_{clay}(c_0 - c_i)} \right) \rho_{dry\ clay}, \quad (1)$$

where,

$N_{clay}$ = mass of buffer lost per unit time (kg $yr^{-1}$)
$Q_{eq}$ = equivalent flow rate ($m^3\ yr^{-1}$)
$c_i$ = $Ca^{2+}$ concentration in groundwater that has reacted with bentonite in the fracture ("leaving groundwater"; mol $m^{-3}$)
$c_w$ = $Ca^{2+}$ concentration in groundwater prior to reaction with bentonite in the fracture ("entering groundwater"; mol $m^{-3}$ )
$c_0$ = concentration of $Ca^{2+}$ that could be added to bentonite porewater by dissolution of soluble minerals (mol $m^{-3}$).
$\varepsilon_{clay}$ = buffer porosity
$\rho_{dry\ clay}$ = dry density of the buffer.

The equivalent flow rate, $Q_{eq}$, in this case represents the flow rate of groundwater that will carry away the $Ca^{2+}$ that diffuses into the groundwater from the buffer's porewater with an average concentration equal to the difference between $c_i$ and $c_w$.

Equation (1) was evaluated by SKB under two limiting conditions regarding the amount of soluble calcite that is assumed to be initially present in bentonite: either 0 or 1 wt%. Any calcite in the buffer is assumed to dissolve completely and instantaneously. Other initial and boundary conditions are:

$Q_{eq}$ = 0.001 $m^3\ yr^{-1}$,
$c_0$ = 10 mol $m^{-3}$ (0 wt% calcite) or 1250 mol $m^{-3}$ (1 wt% calcite),
$c_i$ = CCC = 1 mol $m^{-3}$,
$c_w$ = 0 mol $m^{-3}$,
$\rho_{dry\ clay}$ = 1600 kg $m^{-3}$, and
$\varepsilon_{clay}$ = 0.4.

The results of the calculations indicate $N_{clay}$ = 0.4 kg $yr^{-1}$ for the first case (0 wt% calcite), and $N_{clay}$ = 0.0032 kg $yr^{-1}$ for the second case (1 wt% calcite). If it is assumed that buffer performance could be adversely affected if 1200 kg of bentonite erodes from the fracture/deposition hole (Börgesson and Hernelind, 2006; SKB 2006), then these estimated erosion rates suggest that this could happen within about 3000 to 375,000 years depending on the amount of calcite initially present in the buffer.

Liu and Neretnieks (2006) use a revised version of the conceptual model discussed above to obtain alternative estimates of buffer erosion rates. The revised model differs from the original in two important respects. First, groundwater flow rates are modeled explicitly in the alternative model instead of using the equivalent flow rate (values for $Q_{eq}$ are also calculated using groundwater flow parameters, however). Second, Liu and Neretnieks (2006) assume that Ca concentrations in the buffer's porewaters are controlled by the solubility of trace amounts of gypsum (0.7 wt.%, which is assumed to be a representative value for MX-80 bentonite). In comparison, Ca concentrations in the prototype model were assumed to be controlled by the calcite inventory (*i.e.*, either 0 or 1 wt.%). Gypsum rather than calcite is considered in the alternative model because the solubility of calcite is considered to be too low to sustain Ca concentrations above the CCC. Gypsum solubility in the alternative model is fixed at 9.8 mM.

Liu and Neretnieks (2006) use the FEMLAB program (Comsol, 2004) to solve for the integrated total flux of Ca along the extruded bentonite-groundwater boundary. The flux is then used to estimate the corresponding buffer erosion rate by assuming that the buffer is dispersed as a colloid and lost from the fracture/deposition hole when the concentration of Ca in the buffer's porewater falls below the CCC. Results using "central values" for groundwater flow parameters [hydraulic gradient (0.01), transmissivity ($10^{-8}$ $m^2\ s^{-1}$) and fracture aperture $10^{-4}$ m)] suggest that the erosion rate would be 0.11 kg $yr^{-1}$. This suggests that advective conditions corresponding to a loss of 1200 kg of bentonite would be established within 11,000 years.

## 2.2 Treatment of buffer erosion in SR-Can

The conceptual models described in Section 2.1 were not used to estimate buffer erosion rates in the SR-Can safety assessment (SKB 2006). Rather, the rates were estimated using:

$$R_{buffer} = C_{Max} Q_{eq}, \quad (2)$$

where $R_{buffer}$ stands for the erosion rate (kg yr$^{-1}$), $C_{Max}$ refers to the maximum concentration of bentonite in a water suspension (50 kg m$^{-3}$) and $Q_{eq}$ denotes the equivalent flow rate (m$^3$ yr$^{-1}$). The equivalent flow rate is used to quantify the exchange of solutes between flowing groundwater in the host rock and bentonite in the deposition hole. The model assumes that bentonite consists only of a pure Na-montmorillonite. The value chosen for $C_{max}$ appears to be based on empirical observations.

Representative results obtained using Equation (2) are shown in Figure 2 for a stylized case in which it is assumed that flow conditions at repository depth are similar to those observed at the Forsmark site today (SKB 2006). It is also assumed that these conditions persist for a period of 25,000 years, and that spalling of the host rock near the deposition hole may occur. The estimated total amounts of buffer lost after 25,000 years can be compared to the benchmark value of 1,200 kg marking the threshold value above which advective conditions could be generated in the buffer (Börgesson and Hernelind, 2006). Results are shown for three alternative hydrogeologic models: 1) a fully correlated discrete fracture network (DFN) model; 2) a semi-correlated DFN model; and 3) a continuous porous medium (CPM) model (SKB 2006). The DFN models are generally conservative in the sense that they tend to result in more severe consequences with respect to solute release and transport to and from the geosphere.

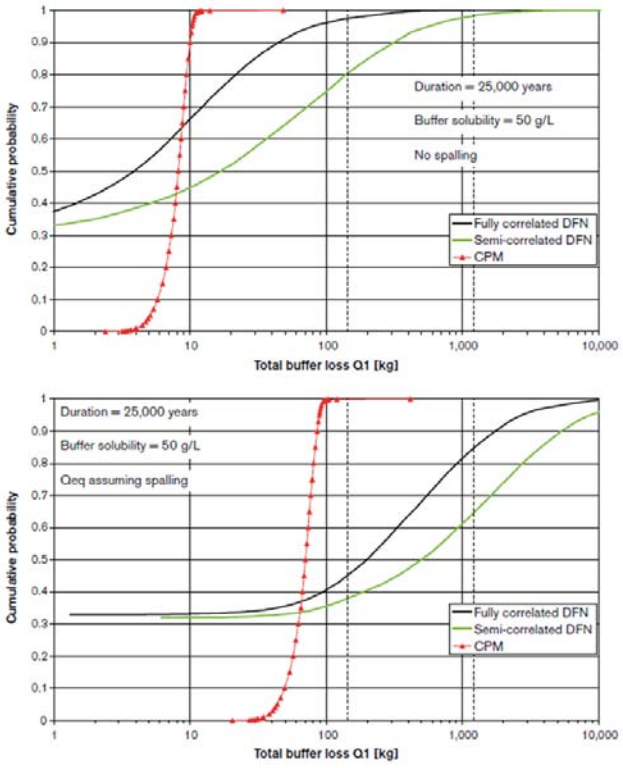


**Figure 2.** Estimated buffer mass losses from deposition holes after 25,000 years (SKB 2006). Equivalent flow rates are estimated based on hydrogeologic modeling of the Forsmark site for temperate conditions similar to those observed at repository depth today (see text). Results are shown for the case of no spalling (upper figure) and spalling (lower figure) of the bedrock near deposition holes.

The results in Figure 2 for the semi-correlated DFN model without spalling indicate that 1200 kg of the buffer would be lost from about 3% of the deposition holes. The alternative flow models predict that buffer losses would be less than 1200 kg in all deposition holes. With spalling, more than 1200 kg of the buffer is predicted to be lost after 25,000 years from 15% of the deposition holes using the fully correlated DFN model, from 35% of the holes using the semi-correlated DFN model and from none of the holes using the CPM model. Similar estimates using the semi-correlated DFN model for the Laxemar site indicate that at least 1200 kg of bentonite would be lost from 40% of the deposition holes after 25,000 years (SKB 2006).

These illustrative results suggest that advective conditions in the buffer could be generated in a substantial number of deposition holes over a reasonable range of hydrogeological conditions at the Forsmark and Laxemar sites. SKB notes, however, that there is considerable uncertainty in the accuracy of erosion rates estimated using Equation (2) (SKB 2006). This is because the calculation model is not built upon a mechanistic understanding of processes controlling colloid release from compacted buffer materials. Repulsive forces acting to separate, and thus stabilize, colloidal suspensions are not considered in the model, for example, and these forces should act to increase the erosion rate (see Section 3.2). On the other hand, SKB notes that preliminary experimental and theoretical evidence suggests that colloid release from commercial

bentonites, especially those in which Ca is an important exchangeable cation in montmorillonite, are much less susceptible to colloid formation than are montmorillonites in the pure Na form (SKB 2006). For these reasons, SKB concludes that it is possible that actual erosion rates for the buffer in a KBS-3 repository could be lower, or higher, than those presently estimated using Equation (2).

# 3 Surface-chemical concepts governing clay colloid formation and stability

*This section considers the theoretical basis of surface-chemical concepts governing the formation and stability of clay colloids. The discussion focuses on the so-called DLVO theory, and refinements and extensions to that theory that have been proposed for aqueous colloidal systems containing clays.*

## 3.1 Colloid terminology

The colloid nomenclature adopted here is largely that recommended by the International Union for Pure and Applied Chemistry (IUPAC; see Everett, 1971). *Colloids* are thus solid particles (*e.g.*, clays) having a length between 1 nm and 1μm in at least one direction. A *colloidal dispersion* is a system in which the colloidal particles are dispersed in a *continuous medium* such as an aqueous solution.

The particles in a *colloidal system* may be discrete or may form continuous network structures having basic units that are in the range of colloidal dimensions. A *sol* is a fluid, or semifluid colloidal system. A *gel* is a colloidal system having a continuous network structure and a finite yield stress. *Repulsive gels* result from electroviscous effects that tend to inhibit colloid movement in systems having low aqueous salt concentrations and high colloid concentrations (Lagaly 2006). *Attractive (or cohesive) gels* form in aqueous solutions having relatively high salt concentrations, which allow attractive forces between colloidal particles to outweigh repulsive forces (see Section 3.2). If the attractive forces become too strong the gel network disintegrates, forming *flocs*, which settle into a sediment.

The distinction between sols, gels and flocs is important because it is generally assumed that the buffer is not susceptible to chemical erosion unless sols are formed[2] (Neretnieks 2008). Stability relations among montmorillonite flocs, sols, attractive gels and repulsive gels are illustrated schematically in Figure 3 as a function of aqueous electrolyte concentration and clay content. These boundaries are somewhat problematic for *thixotropic gels*, which tend to maintain their shape until they are subjected to shearing or some other disturbance. They may then act as a sol and flow freely. Thixotropic behavior is reversible: if undisturbed, and, given enough time, a sol will revert to a gel.

## 3.2 DLVO theory

DLVO is an acronym derived from the surnames of researchers that developed this theory of colloid stability (Derjaguin and Landau, 1941; Verwey and Overbeek, 1948; see also Kruyt 1952; Adamson, 1967; van Olphen, 1977; Sposito 1984; Stumm and Morgan, 1996). The theory is based on electrical properties of the colloid-water interfacial region and on interaction energies that come into play when two charged colloidal particles approach one another.

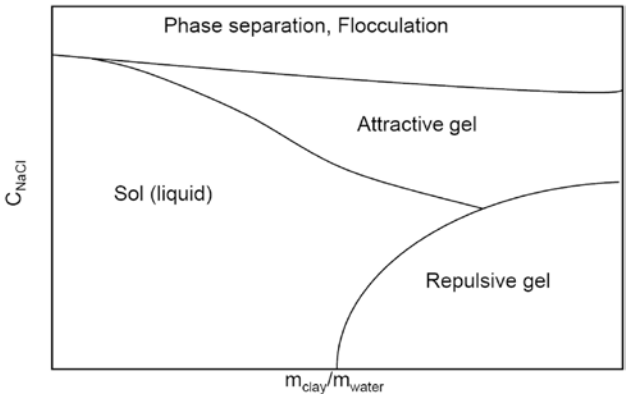


**Figure 3.** Schematic diagram illustrating fields in which clay flocs, attractive gels, repulsive gels and sols are stable as a function of aqueous NaCl concentration and clay/water mass ratio (Hedström et al., 2008).

2 Advective transport of cohesive gels in flowing groundwater is also possible, however.

### 3.2.1 Electrical conditions at the clay-water interface

The electrostatic forces considered in DLVO theory arise from electrical interactions at the solid-liquid interface (Figure 4). For clay colloids a net electrical charge on the particles arises from several sources that can be represented by (Stumm and Morgan, 1996):

$$\sigma_p = \sigma_o + \sigma_H + \sigma_{is} + \sigma_{os} \quad (3)$$

where $\sigma_p$ stands for the net particle charge, $\sigma_o$ denotes the permanent structural charge resulting from isomorphous substitutions on tetrahedral and octahedral sites in the clay's crystalline lattice, $\sigma_H$ refers to the net proton charge resulting from proton-exchange reactions involving ionizable surface hydroxyl groups (represented by S-OH, where S includes Si, Al, *etc.*), $\sigma_{is}$ stands for an inner-sphere complex charge and $\sigma_{os}$ represents an outer-sphere complex charge (all charges have units of C $m^{-2}$). The latter two charges represent contributions to the net particle charge resulting from the specific adsorption of cations and anions by surface hydroxyl groups.

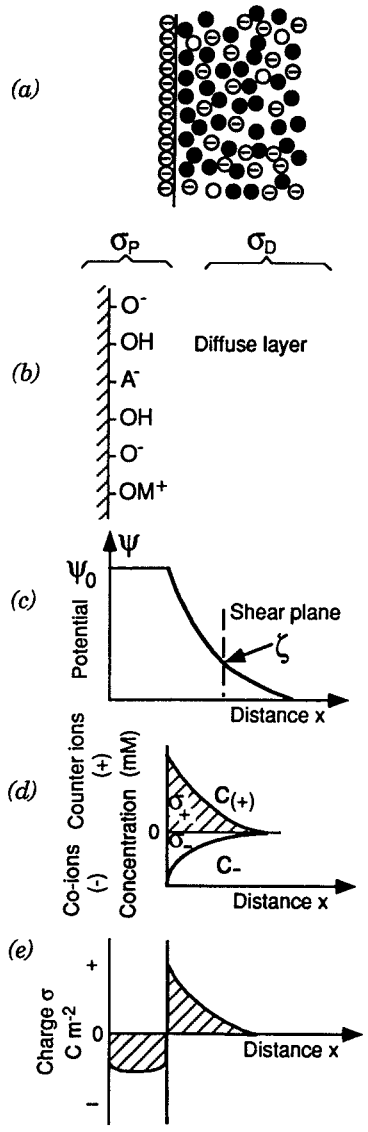


$$\sigma_P = \frac{F}{s}\left[\{S\text{-}OH_2^+\}+\{S\text{-}OM^+\}-\{S\text{-}O^-\}-\{S\text{-}A^-\}\right] \quad \text{(i)}$$

$$\sigma_P + \sigma_D = 0 \quad \text{(ii)}$$

approximately

$$\psi = \psi_0 \exp(-\kappa d) \quad \text{(iii)}$$

$$C_+ = C_{x=\infty} \exp\left(\frac{-zF\psi}{RT}\right) \quad \text{(iv)}$$

$$C_- = C_{x=\infty} \exp\left(\frac{zF\psi}{RT}\right) \quad \text{(v)}$$

$$\sigma_P = (8RT\varepsilon\varepsilon_0 C_x 10^3)^{1/2} \cdot \sinh\left(\frac{zF\psi_0}{2RT}\right) \quad \text{(vi)}$$

**Figure 4.** The diffuse double layer (after Stumm and Morgan, 1996). The diffuseness of the double layer results from thermal motions in the aqueous phase *(a)*. Binding of $H^+$, $O^{2-}$, cations ($M^{2+}$) and anions ($A^-$) can occur on surface sites at the solid-water interface *(b)*. The electric potential ($\psi$) decreases with increasing distance outward into the diffuse layer from the surface, where the potential is $\psi_o$ *(c)*. The zeta potential ($\zeta$) is the potential at the shear plane of a moving particle. Variations in the charge distribution of cations and anions is shown in Figure *(d)*, and Figure *(e)* shows the corresponding net excess charge.

The existence of charged colloidal particles in an aqueous electrolyte solution creates an electrical double layer of charge (Figure 4a,b). One layer corresponds to charges on the particle's surface, as discussed above, and the other is a compensating net charge that is spread out in a diffuse layer extending outward into the aqueous phase. Electrical neutrality in this interfacial region requires that

$$\sigma_p + \sigma_d = 0, \quad (4)$$

where $\sigma_d$ refers to the total net charge in the diffuse layer.

The Gouy-Chapman model of the electrical double layer (*e.g.*, Adamson 1967) establishes a simple relation between particle charge and electrical potential at the particle's surface. It is assumed in this model that the particle's surface is a uniform infinite plane of charge and that aqueous ions exist as point charges in a uniform medium characterized by the dielectric constant. For a symmetrical electrolyte under such conditions the relation between surface charge and surface potential ($\psi_o$; in V) is given by (*e.g.*, Stumm and Morgan, 1996):

$$\sigma_p = (8\varepsilon\varepsilon_o n_s k_B T)^{1/2} \sinh\left(\frac{ze\psi_o}{2k_B T}\right), \quad (5)$$

where $\varepsilon$ denotes the relative dielectric constant of water (78.5 at 25°C), $\varepsilon_o$ represents the permittivity of free space ($8.854 \times 10^{-12}$ C $V^{-1}$ $m^{-1}$), $n_s$ stands for the number of ion pairs ($cm^{-3}$), $k_B$ refers to the Boltzmann constant ($1.3805 \times 10^{-23}$ J $K^{-1}$), $T$ denotes temperature (K), $z$ represents ionic valence, and $e$ stands for the elementary charge ($1.60219 \times 10^{-19}$ C). At 25°C, Equation (5) becomes:

$$\sigma_p = 0.1174 c_s^{1/2} \sinh\left(\frac{ze\psi_o}{2k_B T}\right) \quad (6)$$

where $c_s$ refers to electrolyte concentration (M). Note that if $\psi_o$ << 25 mV at 25°C,

$$\sigma_p = 2.5 I^{1/2} \psi_o \quad (7)$$

where $I$ refers to ionic strength (M).

The potential at the particle's surface decreases with increasing distance, $x$, outward from the surface into the diffuse layer. The potential at any point in the diffuse layer can be calculated using:

$$\frac{d^2\psi}{dx^2} = \frac{\kappa^2 \sinh\left(\frac{ze\psi}{k_B T}\right)}{\left(\frac{ze}{k_B T}\right)}, \quad (8)$$

where $\kappa$ represents the reciprocal thickness of the double layer given by:

$$\kappa = \left(\frac{e^2 \sum_i n_i z_i^2}{\varepsilon\varepsilon_o k_B T}\right)^{1/2}, \quad (9)$$

and where $n_i$ stands for the number concentration ($cm^{-3}$) of ions with valence $z_i$. A simplified version of Equation (8) that is valid when $\psi$ << 25 mV is given by:

$$\frac{d^2\psi}{dx^2} = \kappa^2 \psi, \quad (10)$$

in which case,

$$\psi = \psi_o e^{(-\kappa x)} \quad (11)$$

and the potential thus decays exponentially at a rate that increases with decreasing thickness of the double layer (*i.e.*, with increasing values of $\kappa$).

Once the spatial distribution of electrical potentials in the diffuse layer is known, corresponding ionic concentrations can be calculated using the Boltzmann equation for cations and anions (*e.g.*, Adamson 1967):

$$n_+ = n_o e^{(-ze\psi/k_B T)}, \text{ and} \quad (12)$$

$$n_- = n_o e^{(ze\psi/k_B T)}, \quad (13)$$

where $n_+$ and $n_-$ represent local concentrations (mol $cm^{-3}$) of cations and anions in the diffuse layer, respectively, and $n_o$ stands for ion concentrations in the bulk solution (*i.e.*, where $n_+ = n_-$ by charge balance). These local concentrations are important because, as discussed in the following section, they affect repulsive forces resulting from the interactions of double layers when two colloidal particles approach one another.

### 3.2.2 Interaction energies among colloidal particles

DLVO theory assumes that the stability of an aqueous colloidal system is controlled by a balance between electrostatic forces, which tend to repel particles of like charge, and attractive forces arising from van der Waals interactions. The concept is illustrated in Figure 5, which depicts changes in the total interaction energy, $V_T$, as two colloidal particles approach one another due to thermally driven Brownian motion. The net interaction energy represents the sum of electrostatic double-layer

repulsion ($V_R$) and van der Waals attraction ($V_A$) energies, *i.e.*,

$$V_T = V_R + V_A \tag{14}$$

At very small interparticle distances an additional repulsive force, indicated by the dotted line in Figure 5, arises due to the interaction of atomic electronic clouds (Born repulsion). Colloids are stable when $V_T > 0$ and unstable when $V_T < 0$.

In general, approximate solutions to Equation (14) must be sought for realistic colloidal systems. Exact solutions are available, however, for idealized cases in which the particles are represented by parallel flat plates or spheres. These solutions are discussed below because they entail considerations that must generally be made in models of clay colloid stability.

**3.2.2.1 Colloids as parallel flat plates.** Kruyt (1952) (see also Adamson 1967; Jansson 2007) derives a solution for the repulsive term in Equation (14) for an idealized case in which colloidal particles are assumed to be parallel flat plates (Figure 6). The total force acting on the plates consists of an osmotic pressure force and a force arising from the electrical field. The latter force equals zero at the midplane ($m$) between the plates (*i.e.*, at $x = d/2$ in Figure 6) because $d\psi/dx = 0$ at that location. The total force is thus given by the osmotic pressure at the midplane position.

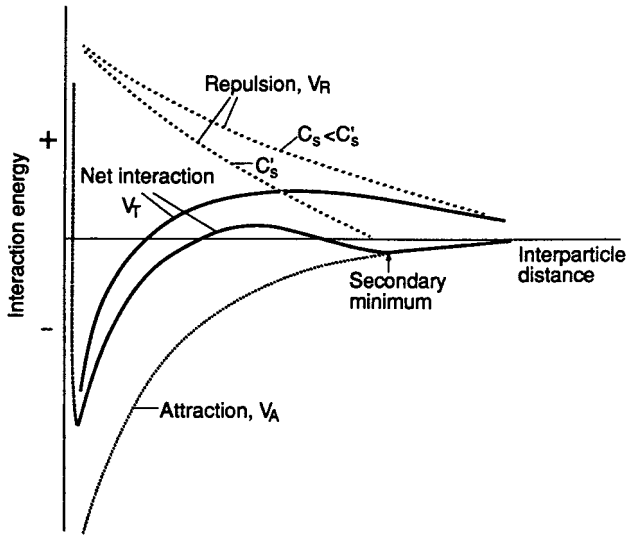


**Figure 5.** Schematic diagram illustrating the relation between interaction energies and separation distances between colloidal particles (see text; after Stumm and Morgan, 1996).

The osmotic pressure, $\Delta p$, is given by:

$$\Delta p = p_m - p_o = n_{excess} k_B T = \left[ n_o \left( e^{\frac{ze\psi_m}{k_B T}} + e^{\frac{-ze\psi_m}{k_B T}} \right) - 2n_o \right] k_B T \tag{15}$$

where $p_m$ and $p_o$ refer to pressures at the midplane and bulk aqueous phase, respectively, and $n_{excess}$ stands for the excess concentration of cations and anions at $m$ relative to their concentrations in the bulk solution. The expression on the right-hand side of the second identity in Equation (15) is obtained using Equations (12) and (13), and $\psi_m$ refers to the midplane potential. Integration of Equation (15) between $\psi = 0$ to $\psi = \psi_m$ yields (Kruyt 1952):

$$\Delta p = 2n_o k_B T[\cosh(ze\psi_m / k_B T) - 1] \tag{16}$$

This osmotic pressure represents the force per unit area driving colloidal particles apart as a consequence of interactions involving their electrical double layers.

Integration of Equation (16) to obtain the total repulsive energy, $V_R$, in Equation (14) can be difficult because $\psi$ generally varies as a complex function of distance between the colloidal particles. Kruyt (1952) notes, however, that for the case of relatively weak interactions between the particles (*e.g.*, when

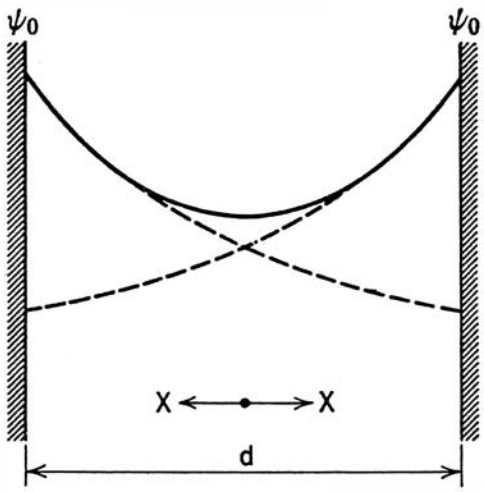


**Figure 6.** Interacting double layers between the surfaces of two colloidal particles represented by parallel flat sheets. (Adamson 1967). Potentials in the double layer adjacent to each sheet are shown as a function of distance from the surface, d, by the dashed lines. The solid line represents the total potential resulting from the interacting double layers.

$\psi_m << 1$ V), the following relation can be used:

$$\frac{ze\psi_m}{k_B T} = 8\gamma e^{-\kappa m}, \quad (17)$$

where,

$$\gamma = \frac{(e^{\frac{ze\psi_o}{k_B T}} - 1)}{(e^{\frac{ze\psi_o}{k_B T}} + 1)}. \quad (18)$$

Equation (17) can be used in a first approximation[3] to Equation (16) to obtain:

$$\Delta p = n_o k_B T (8\gamma e^{-km})^2, \quad (19)$$

which can then be integrated from $x = \infty$ (bulk solution) to $x = m$ to yield (Kruyt 1952):

$$V_R = -2\int_{x=\infty}^{x=m} \Delta p dx = \frac{64 n_o k_B T}{\kappa}\gamma^2 e^{-2\kappa m}. \quad (20)$$

Equation (20) gives the total repulsive energy between colloidal particles for an idealized case in which the particles are represented by parallel flat plates.

DLVO theory attributes the attractive term, $V_A$, in Equation (14) to van-der Waals-London dispersion forces. These can be calculated in principle using Lifshitz theory (Lifshitz 1956), which accounts for the macroscopic electrodynamic properties of the interacting media. In practice, however, relatively simple expressions for $V_A$ are usually derived using an alternative approach developed by Hamaker (1937). In this approach the attraction energy between two bodies is calculated as the sum of London dispersion interactions among all pairs of atoms in the two bodies. The approach is valid as long as separations between the bodies do not approach atomic dimensions.

Using Hamaker's approach, $V_A$ for two colloidal particles represented by parallel flat sheets can be calculated using (*e.g.*, Kruyt 1952):

$$V_A = -\frac{A}{48\pi m^2}, \quad (21)$$

where $A$ denotes the Hamaker constant (J) and $m$, as noted earlier, stands for the midplane position (*i.e.*, $m = d/2$, where $d$ represents the separation distance between the particles as shown in Figure 6). Values for the Hamaker constant are difficult to determine experimentally. For clay colloids, $A \approx 10^{-20}$ J appears to be a reasonable value (*e.g.*, Lyklema 1991; Swanton 1995; Helmy 1998).

3 Note that $\cosh(x) \approx 1 + x^2/2$ when x is small.

Substituting Equations (20) and (21) into Equation (14) results in:

$$V_T = \frac{64 n_o k_B T}{\kappa}\gamma^2 e^{-2\kappa m} - \frac{A}{48\pi m^2}, \quad (22)$$

which gives the net total interaction energy between sheet-like colloidal particles as they approach one another. As is illustrated schematically in Figure 5, the net interactions are repulsive at relatively large particle separations, but become attractive when the particles reach a threshold separation that depends on the aqueous electrolyte concentration. The relation between this threshold distance and the critical coagulation concentration (CCC) of aqueous ionic species is considered further in Section 3.3.

**3.2.2.2 Colloids as spherical particles.** Garcia-Garcia *et al.* (2007; 2009; see also Kruyt 1952; Stumm and Morgan, 1996) derive equations for the case of idealized spherical colloidal particles that are analogous to Equations (20) and (21) for parallel flat plates. Garcia-Garcia *et al* (2007) believe that adopting a spherical rather that planar geometry is more reasonable for clay particles, which tend to have irregular shapes built up from flat surfaces oriented in many different directions. The resultant expression for the repulsive term in Equation (14) is given by:

$$V_R = \frac{64\pi r_p n_o k_B T}{\kappa^2}\gamma^2 e^{-\kappa d}, \quad (23)$$

where $r_p$ stands for particle radius (assumed to be the same for both interacting particles), $n_o$ denotes the number of ions ($m^{-3}$) and $d$ refers to the separation distance between the particles (*i.e.* this is twice the value of the midplane position, $m$, considered in Eqn. (20)). The parameters $\kappa$ and $\gamma$ in the above equation are conceptually similar to their counterparts for the case of parallel flat plates (Eqns. (9) and (18), respectively), and are given by (*e.g.*, Garcia-Garcia *et al.*, 2009):

$$\kappa = \left(\frac{1000 e^2 N_a \sum_i z_i^2 M_i}{\varepsilon\varepsilon_o k_B T}\right)^{1/2}, \text{ and} \quad (24)$$

$$\gamma = \frac{(e^{\frac{ze\psi_o}{2k_B T}} - 1)}{(e^{\frac{ze\psi_o}{2k_B T}} + 1)}, \quad (25)$$

where $N_a$ stands for Avogadro's number and $M_i$ represents the molarity of the $i$-th ion with valence $z_i$. The parameter $\kappa$ provides a measure of the inverse thickness of the diffuse layer adjacent to a particle's

surface (see Section 3.2.1) and γ varies only with the magnitude of the surface potential at a given temperature.

An expression for the attractive van der Waals force among spherical particles (Eqn. (14)) that is analogous to that for planar geometry (Eqn. (21)) is given by (Garcia-Garcia *et al.*, 2009):

$$V_A = \frac{-A}{6}\left(\frac{2r_p^2}{d^2+4r_p d}+\frac{2r_p^2}{(d+2r_p)^2}+\ln\left(\frac{d^2+4r_p d}{(d+2r_p)^2}\right)\right) \quad (26)$$

This expression indicates that the attractive force is strongly dependent on particle size, in distinct contrast to the corresponding expression for planar geometry (Eqn. (21)). Values for the Hamaker constant apparently do not vary significantly with particle geometry.

Substituting Equations (23) and (26) into Equation (14) results in:

$$V_T = \frac{64\pi r_p n_o k_B T}{\kappa^2}\gamma^2 e^{-\kappa d} - \frac{A}{6}\left(\frac{2r_p^2}{d^2+4r_p d}+\frac{2r_p^2}{(d+2r_p)^2}+\ln\left(\frac{d^2+4r_p d}{(d+2r_p)^2}\right)\right) \quad (27)$$

which gives the total interaction energy between spherical colloidal particles. As is illustrated schematically in Figure 5, the net interactions are repulsive at relatively large particle separations, but become attractive when the particles reach a threshold separation that depends on the aqueous electrolyte concentration. This dependence of $V_T$ on ionic strength is considered further below.

## 3.3 Effects of aqueous chemistry and temperature on colloid stability

The effects of electrolyte concentration on colloid stability are illustrated in Figure 5 by the two dashed curves showing variations in $V_R$ as a function of interparticle distance, and corresponding solid curves for $V_T$. Electrolyte concentration $C_s$ is assumed to be smaller than $C_s^*$, and the diagram therefore indicates that colloidal suspensions (of planar or spherical geometry) are stable (*i.e.*, $V_T > 0$) over a broader range of inter-particle distances as the aqueous medium becomes more and more dilute. The secondary minimum in $V_T$ when the electrolyte concentration equals $C_s^*$ results in the formation of an attractive gel, which may re-disperse (peptize) as a sol by stirring.

Separation distances among the particles in an aqueous colloidal suspension depend on the ionic strength of the medium because this parameter determines how the electrical potential decays with increasing distance outward from the surface into the double layer[4]. As noted in Section 3.2, the thickness of the double layer is generally taken as being equal to the reciprocal of the (Debye) parameter, κ, which is recast here as:

$$\kappa = \left(\frac{2F^2 I \times 10^3}{\varepsilon\varepsilon_0 RT}\right)^{1/2}, \quad (28)$$

where $F$ refers to the Faraday constant, $I$ represents ionic strength, given by

$$I = 1/2\sum_i z_i^2 M_i, \quad (29)$$

and $R$ stands for the gas constant. This equation indicates that the thickness of the double layer must decrease as ionic strength increases, and this allows the individual particles in a colloidal suspension to move closer together. The particles will eventually form an attractive gel or floc if the double-layer thickness falls below a value corresponding to a threshold separation distance at which $V_T$ first becomes negative. Conversely, stable colloids may form from a gel or floc if the ionic strength decreases to a point where $V_T$ becomes positive. Chemical erosion of the buffer is thus more likely in situations where the buffer comes into contact with groundwaters that are relatively dilute.

The concept of a critical coagulation concentration (CCC) discussed in Section 2.1 can be related to compositional constraints on the aqueous phase that come into play when the threshold separation distance between colloidal particles is reached (*i.e.*, when $V_T = 0$). Considering the idealized case of colloids as parallel flat plates, for example, Equation (22) indicates that under such conditions

$$\frac{64 n_o k_B T}{\kappa}\gamma^2 e^{-2\kappa m} = \frac{A}{48\pi m^2}. \quad (30)$$

Kruyt (1952) rearranges this equation to give at 25°C

$$c = 8\times10^{-22}\frac{\gamma^4}{A^2 z^6}, \quad (31)$$

4 Van der Waals interactions are not affected by ionic strength.

where $c$ represents electrolyte concentration (mM) and where it is assumed that surface potentials in the expression for $\gamma$ (Eqn. (18)) are sufficiently high that $\gamma \approx 1$ and is independent of valency. The electrolyte concentration, $c$, is taken to be a critical coagulation concentration at, and below, which attractive forces between colloidal particles dominate, leading to the formation of attractive gels or flocs.

The prediction in Equation (31) that the CCC should vary according to an inverse 6-th power dependence on electrolyte valence is in reasonably good agreement with many empirical observations and is known as the rule of Schulze and Hardy (*e.g.*, Stumm and Morgan, 1996). When extended to systems in which the surface potential is low and $\gamma$ (Eqn. (18)) $\neq 1$, the Schulze-Hardy rule invokes a $(1/z)^2$ dependence on valence (Kruyt 1952). In either case, for negatively charged colloids such as clays, the CCC for cations tends to decrease strongly in the order monovalent > divalent > trivalent. Thus, although monovalent cations such as $Na^+$ or $K^+$ tend to be more abundant in natural waters than divalent cations, such as $Ca^{2+}$ or $Mg^{2+}$, the latter cations are expected to more strongly influence colloid stability than the former due to the Schulze-Hardy rule. It is important to emphasize, however, that this rule applies only to electrolytes that are "indifferent", *i.e.*, they do not react with other ions in the double layer and are not specifically adsorbed at the colloid's surface. Trivalent cations, such as $Al^{3+}$ and $Fe^{3+}$, generally have very low concentrations in natural waters due to solubility constraints, and may not behave like indifferent electrolytes with respect to clay minerals.

It is not obvious how changes in temperature might affect colloid stability because relations among variables controlling colloid stability are complex, even for the case of idealized systems (Section 3.2). Garcia-Garcia *et al.* (2009) note that increases in temperature can increase or decrease the stability of clay colloids depending on the pH and ionic strength of the aqueous phase. An increase in temperature generally increases the kinetic energy and frequency of collisions among colloidal particles, and this will tend to favor the formation of flocs or gels. An increase in pH at a given temperature will increase the net negative charge/potential on clay colloids and this will tend to increase the repulsive energy between particles. Increasing the ionic strength at a given temperature promotes flocculation because it tends to reduce the thickness of the double layer, as discussed above. Overall, Garcia-Garcia *et al.* (2009) note that at low surface potentials repulsion between clay particles decreases with increasing temperature, and at high surface potentials repulsion increases with increasing temperature. The latter increase in repulsion with increasing temperature may counteract the attendant increase in collision frequency and energy, causing a colloidal system to stabilize.

# 4 Uncertainties in surface-chemical concepts applied to models of buffer erosion

*This section considers uncertainties in models of buffer erosion that stem from conceptual deficiencies in understanding surface-chemical constraints on the stability of clay colloids. The discussion considers deficiencies in DLVO theory and the effects of ion exchange on stability relations among montmorillonite sols, gels and flocs.*

## 4.1 Deficiencies in DLVO theory applied to clay colloids

There is a general consensus that the conceptual basis of DLVO theory is substantially correct, but that the theory is also deficient in some important respects (*e.g.*, Kruyt 1952; Swanton 1995; Stumm and Morgan, 1996; Missana and Adell, 2000; Boström *et al.*, 2001; McBride and Baveye, 2002). Support for this view comes from studies involving direct force-balance measurements (see Iraelachvili and Adams 1978; Israelachvili 1991) of adhesive and repulsive interactions among colloidal particles (see Swanton 1995). These studies suggest that the treatment of van der Waals interactions in the DLVO model is generally valid as long as separation distances between colloidal particles are greater than atomic dimensions. The treatment of electrical double-layer interactions (Section 3.2.2) also appears to be valid, although important discrepancies between model predictions and experimental observations have been noted in some systems, especially those with divalent electrolytes (*e.g.*, Section 4.2).

Limitations in DLVO theory arise for two general reasons: 1) oversimplification of the properties of real colloids, and 2) omission of "non-DLVO" forces that can be important under certain circumstances. These limitations can be categorized as follows (Swanton 1995):

- The theory treats colloidal particles as if they were smooth bodies having ideal geometries. Real colloids are irregular in size and shape, however, and have rough surfaces. Surface roughness can affect both the attractive van der Waals interactions as well as repulsive double-layer forces.
- Surface charge/potential is assumed to be uniformly distributed. Charges are discrete by nature, however, and electrical properties of colloidal particles can therefore vary on a microscopic scale. Such heterogeneous distributions of surface charge/potential could affect the magnitude of repulsive double-layer interactions.
- DLVO theory does not consider interactions involving the solvent, which is treated as a continuous homogeneous medium characterized by a single value of the dielectric constant. Such interactions could arise, however, if the solvent is polar [as is $H_2O(l)$]. For aqueous systems, these interactions may include hydrogen bonding, hydrogen donor/acceptor reactions, hydration and steric interactions. The result of such interactions is a re-structuring of water in layers adjacent to the solid's surface.
- Ions in the diffuse layer are assumed to be point charges, *i.e.*, the sizes of the ions are ignored. This assumption is not valid when the separation distance between colloidal particles is small and the surface potential is high. Under such conditions, the numbers of ions in the diffuse layer calculated using DLVO theory are far too large.
- Repulsive and attractive forces between colloidal particles are assumed not to vary with time. In reality, however, the total interaction energy between particles may fluctuate due to a redistribution of charge in the double layer or solid by diffusive or conductive mechanisms, or during particle rotations as a result of irregular particle shape and/or heterogeneities in surface charge.

Swanton (1995) (see also Jansson 2007) describes recent efforts to deal with these limitations. These efforts have resulted in the formulation of various "extended" DLVO models. The extended models provide more accurate descriptions of colloidal systems,

but come at the expense of an increased number of model parameters that must be characterized experimentally.

There are additional limitations in DLVO theory when it is applied specifically to colloidal systems involving the clay minerals in bentonite (Stumm and Morgan, 1996; Liu and Neretnieks, 2006). One limitation stems from the fact that these minerals carry a net negative charge on faces oriented parallel to the dominant tetrahedral–octahedral–tetrahedral layering, and, depending on pH, net positive or negative charges on edges that are oriented normal to this layering (*e.g.*, Grim, 1968). This means that a given clay particle can have different double-layer structures associated with its faces and edges. Particle-particle interactions in clay colloidal systems may consequently involve face–to–face (FF), edge–to–face (EF) and edge–to–edge (EE) interactions. Because the EF interactions involve particle surfaces of unlike charge, particle agglomeration may occur even in dilute electrolyte solutions. The DLVO model does not account for such interactions, and may thus overestimate the stability of clay colloids.

The DLVO model also does not account for the effects of specific adsorption on colloid stability (Boström *et al.*, 2001). The model assumes only that the electrolytes in a colloidal suspension are inert, and that their effect on colloid stability is through the control on double-layer thickness represented by the reciprocal of the Debye parameter, $\kappa$ (Section 3.3).

Other electrolytes in clay colloidal systems may form covalent complexes with functional groups at a particle's surface, however (*e.g.*, Langmuir, 1997). Such complexes alter the surface charge and surface potential, and thereby affect colloid stability. Hydrogen and $OH^-$ are important potential-determining ions because they react with the surface sites on clay minerals. The colloidal stability of these minerals is thus pH-dependent, but this dependency is not accounted for in DLVO models (Missana and Adell, 2000).

## 4.2 Effects of clay composition on stability relations among sols, gels and flocs

Kjellander *et al.* (1988) use a statistical mechanical approach to evaluate double-layer interactions involving clay minerals. Counter to expectations based on DLVO theory, the interaction energy between like-charged clay surfaces was found to be strongly attractive at relatively small inter-particle separation distances if the counterions in the diffuse layer are divalent and if the surface-charge density is large (as is true generally for smectites, including montmorillonites, see Birgersson 2007).

This additional attractive force is attributed by Kjellander *et al.* (1988) to ion-ion correlations (see also Janiak *et al.*, 2008; Pegado *et al.*, 2008). The correlations involve repulsive interactions among ions of like charge, which in effect create a "hole" of charge depletion around each ion. The charge-depletion region around an ion can be regarded as a charge-accumulation region of opposite sign. The interaction of an ion on one side of the midplane between two colloidal particles (*e.g.*, at $d/2$ in Figure 6) with an ion and part of a charge-depletion hole on the other side of the midplane creates an attractive force between the particles that is not accounted for in classical DLVO theory. This attractive force, together with the van der Waals force, is not large enough to counteract the repulsive force between two clay particles when the counterions are monovalent, but can counteract this repulsive force when the counterions are divalent and the surface-charge density is high.

The attractive force due to ion-ion correlations is apparently important for montmorillonites having exchangeable Ca/Na molar ratios greater than about 90/10 (*e.g.*, Birgersson *et al.*, 2008). In such cases the attractive force is sufficiently strong that the minerals cannot expand to form cohesive gels or sols. On the other hand, montmorillonites having Ca/Na < 90/10 can form cohesive gels or sols depending on whether counterion concentrations exceed the CCC. This is important from the viewpoint of buffer chemical erosion because it suggests that buffer materials composed of essentially pure Ca-montmorillonites would be much more resistant, if not completely impervious, to the effects of chemical erosion than buffer materials composed of mixed Na/Ca-montmorillonites having Ca/Na < 90/10 (e.g., MX-80).

Birgersson *et al.* (2008) use mass-action and mass-balance constraints on ion-exchange reactions to interpret stability relations among montmorillonite sols, gels and flocs. Flocs are predicted to be stable when Ca/Na > 90/10 and aqueous $Na^+$ concentrations are low. Cohesive gels are predicted

to be stable when the ionic strength > 25 mM and Ca/Na < 90/10. Sols are predicted to be stable under these conditions when the ionic strength < 25 mM.

The predicted stability field of sols is quite small and occurs over a range of very low $Na^+$ and $Ca^{2+}$ concentrations[5]. This range may be compatible with the compositions of glacial meltwaters, however, which suggests that even essentially pure Ca-montmorillonites could be susceptible to chemical erosion should they be used as buffer materials in a KBS-3 repository. Any strategy to mitigate the potential effects of chemical erosion by choosing bentonites composed of Ca-montmorillonite rather than mixed Na/Ca- or Na-montmorillonite will likely also have to contend with the possibility that ion-exchange reactions, occurring over time scales of hundreds-of-thousands of years, could significantly alter these Ca-montmorillonites to more sodic forms.

5 Recent experiments suggest that this field is even smaller than predicted (Birgersson *et al*., 2008).

# 5 Supplementary erosion considerations

*This section considers the concept of buffer erosion in relation to STUK's requirements for nuclear waste disposal as specified in Guide YVL D.5. The discussion addresses how buffer erosion could adversely impact safety functions of this engineered barrier, and whether current models of buffer erosion provide a defensible scientific basis for assessing these impacts.*

## 5.1 Recent developments in modeling buffer erosion

Apted et al. (2010) summarized recent developments in buffer-erosion modeling. The following discussion is based on their summary. A conceptual model of buffer erosion is illustrated in Figure 7. The figure represents a vertical cross section through a portion of a KBS-3V deposition hole that is intersected by a horizontal fracture. Free swelling of bentonite from the deposition hole outward into the fracture is resisted by friction forces acting within the bentonite and at the rock interface. The maximum penetration distance is reached when these counteracting forces equilibrate. Bentonite density and swelling pressure then decrease rapidly with increasing distance in the fracture. The rheological properties of the bentonite change accordingly from those of a solid → gel → fluid (which may also include a semi-fluid phase). Fluid properties are identical to those of groundwater at the penetration front. Clay colloids form near this front, and are lost by diffusion into the flowing groundwater. Bentonite fluids (*i.e.*, dispersions of bentonite colloids in water, not solids or gels) may also be lost by advection. More bentonite then extrudes into the fracture from the deposition hole to restore equilibrium. The resultant mass loss of bentonite from the deposition hole results in a decrease in buffer density.

Early models of buffer erosion (Section 2) assumed that clay particles would be swept away by water flowing in a fracture, but the actual mechanisms involved were not specified. Neretnieks *et al.* (2009) recently extended these models to account for forces that would control the expansion of bentonite from the deposition hole into a fracture (dynamic force-balance model), and for the effects of particle and ionic concentrations on the viscosity of the expanded bentonite sols (viscosity model).

The force-balance model assumes that the expansion of the buffer from a deposition hole into an intersecting fracture will be controlled by a number of forces acting on the individual clay particles in bentonite (Neretnieks *et al.*, 2009). The model accounts for the gravity and buoyant force, forces

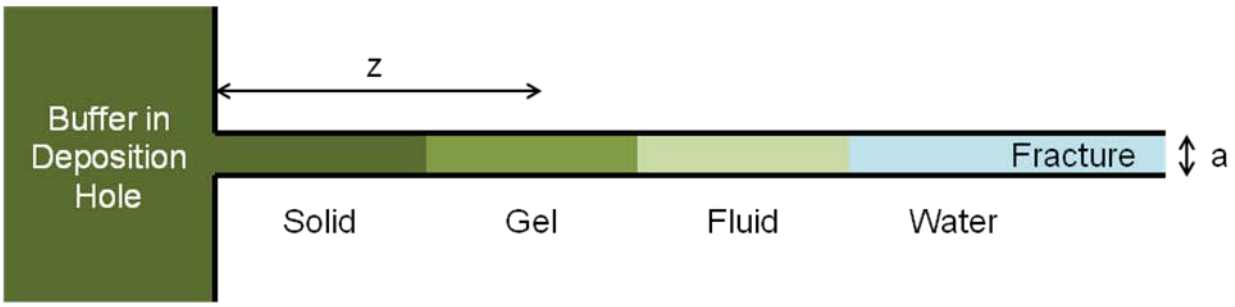


**Figure 7.** Conceptual model of buffer erosion (Birgersson et al., 2009). The swelling pressure of bentonite in the fracture decreases exponentially with increasing distance, z, and, at a given distance, with decreasing fracture aperture, a.

resulting from changes in the chemical potential in a concentration gradient (diffusional force), van der Waals attractive forces between clay particles, repulsive forces between the particles resulting from charges within and on the surfaces of the particles (diffuse double layer forces), and friction forces acting on the particles as they move through the aqueous phase as a result of imbalances among the other forces. Because changes in particle velocity are expected to be slow as the buffer expands into a fracture, acceleration can be neglected and the sum of the forces must then always be equal to zero. Chemical aspects of the force-balance model are mainly incorporated in the attractive van der Waals and repulsive double-layer forces between individual clay particles. These forces are considered in detail in Section 3.

The force-balance model can be used to predict changes in the density and volume fraction of clay particles (φ) as the bentonite expands into a fracture. A complementary viscosity model was developed by Neretnieks *et al.* (2009) to relate changes in φ to corresponding changes in the viscosity of bentonite sols. The viscosity model is based on the concept of a co-volume of a colloidal particle. The co-volume is defined as the volume over which a given particle can rotate freely without touching other particles in a colloidal suspension. It is determined both by the physical size of the particle as well as by interactions involving the particle's electrical double layer and those of its nearest neighbors (see Section 3). The co-volume thus depends on the physical volume fraction (φ) and on properties of the colloidal suspension, such as the ionic composition of the aqueous phase, that control the effective thickness of the electrical double layer.

The force-balance and viscosity models were combined by Neretnieks *et al.* (2009) into an overall model of buffer erosion, which accounts for both the diffusion of individual clay colloids into the flowing groundwater and for the advection of sols that form within the fracture as the bentonite expands and becomes less dense and less viscous. The model was evaluated for an idealized case of two-dimensional groundwater flow in a horizontal fracture intersecting a deposition hole in a KBS-3V repository. The fracture aperture was assumed to be 1 mm. Bentonite was assumed to consist of pure Na-montmorillonite and the groundwater was represented by a dilute NaCl solution. The Darcy flow equation, solute diffusion equations, and governing equations underpinning the force-balance and viscosity models were evaluated simultaneously using a numerical approach and solver. Model results indicated that the erosion rate is proportional to the water velocity raised to the power 0.41, and that the erosion rate increases, and the length of the fracture penetrated by bentonite decreases, with increasing groundwater velocity. Neretnieks *et al.* (2009) note that these results are preliminary and that the erosion rate for a given water velocity could be higher or lower than predicted by the model because the effects of ion transport on the viscosity of bentonite sols have not been adequately accounted for in systems containing both $Na^+$ and $Ca^{2+}$ ions.

## 5.2 Potential impacts of buffer erosion on safety functions and performance targets

Erosion could adversely impact safety functions of the buffer because corresponding performance targets generally depend, either directly or indirectly, on the buffer's density. A case in point that was considered in detail in the SR-Can safety assessment (SKB 2006) is illustrated in Figure 8, where swelling pressure ($p_{swell}$) measurements for an MX-80 bentonite are plotted as a function of dry density and molar NaCl concentrations in the coexisting aqueous solution. It was assumed in SR-Can that advective transport conditions in the buffer could be generated if $p_{swell} < 100$ kPa. As can be seen in Figure 8, such low swelling pressures correspond to dry

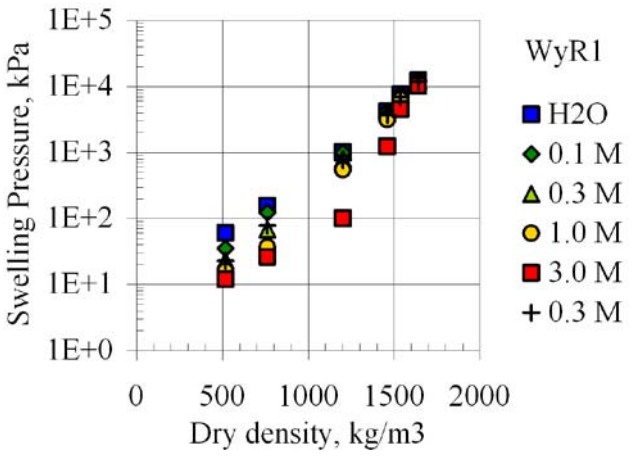


**Figure 8.** Plot showing variations in the swelling pressure of MX-80 bentonite as a function of dry density and aqueous NaCl concentration (Karnland 1997). The montmorillonite component of the bentonite was in the Na-exchanged form.

densities less than about 1000 kg $m^{-3}$. As discussed before, Börgesson and Hernelind (2006) determined that a loss of as little as 1200 kg of bentonite from a deposition hole, represented in their model by the complete loss of the half-circumference of two bentonite emplacement rings, would be sufficient to locally lower $p_{swell}$ below the threshold value of 100 kPa. Although there is some uncertainty in this analysis regarding the assumed nature of friction forces acting between the buffer and rock, the results suggest that at higher mass losses adequate swelling pressure cannot be guaranteed and that advection in the buffer could therefore occur. This is a concern primarily because advection could increase the transport rate of corrodants to the canister's surface, thus potentially decreasing the containment lifetime of this engineered barrier.

The above example considered the impacts of buffer erosion only in terms of the effects of a loss of density on the swelling pressure ($p_{swell}$) and associated effects on the buffer's functional requirement to limit advective transport. It is worth noting, however, that buffer density and $p_{swell}$ also relate to the ability of the buffer to effectively eliminate microbial activity, to prevent canister sinking, and to allow gases produced within a potentially damaged canister to migrate out of the buffer without causing irreversible damage to the buffer's physical properties (Figure 9). Similarly, the buffer's density controls the ability of the buffer to protect the canister from the effects of rock shear, as well as the hydraulic and thermal conductivity of this engineered barrier. It is interesting to note in Figure 9 that mass losses leading to a reduction

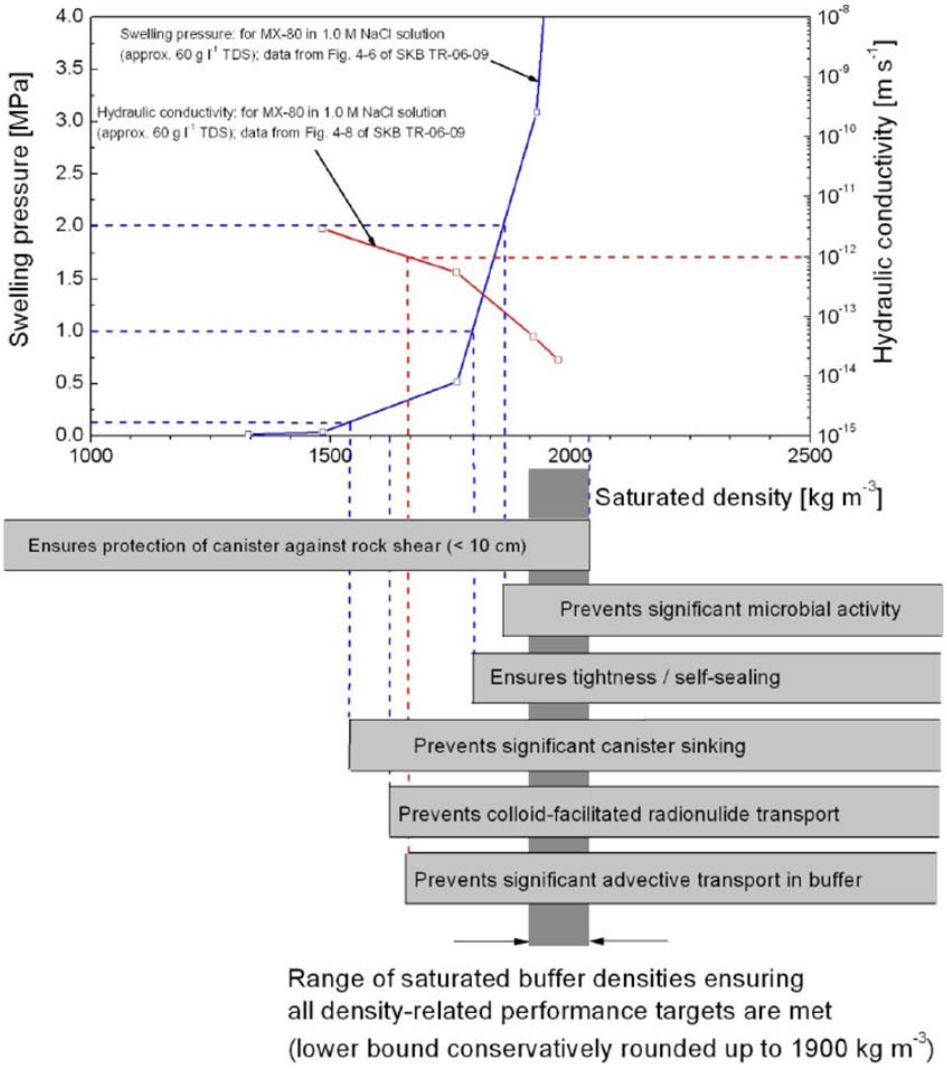


**Figure 9.** Schematic illustration of the effects of buffer saturated density on the swelling pressure, hydraulic conductivity, and related performance targets (Posiva 2010).

in saturated density would impact two performance targets (prevent significant microbial activity and ensure tightness/self-sealing) before they would impact the threshold for significant advective transport to occur. The potential impacts of buffer erosion on repository safety thus depend in a complex and sequential manner on the amount of buffer mass that is lost from a deposition hole.

## 5.3 Possible issues in dealing with buffer erosion in a safety case

There are a number of conceptual uncertainties in current models of buffer erosion (Section 5.1) that are relevant to repository safety (Section 5.2). These uncertainties are considered further below.

### 5.3.1 Mass-loss tolerances

Buffer erosion entails consideration of the amount of buffer mass loss that can be tolerated before safety functions and performance targets would be adversely impacted. Such considerations may be complicated by significant conceptual uncertainties, however. The conclusion in SR-Can that 1200 kg of bentonite can be lost from a deposition hole before advective conditions would be established in the buffer, for example, is based on an analysis that is subject to considerable uncertainty regarding the nature of friction forces acting within the buffer and at the buffer-rock interface (Börgesson and Hernelind, 2006). These uncertainties bring into question whether the buffer would homogenize quickly and completely throughout the deposition hole following a loss of mass by erosion, or whether the effects of mass loss would be localized in the near vicinity of the fracture intersection with the buffer for long periods of time. Independent evaluations by STUK may be needed to determine whether criteria established for unacceptable mass losses of the buffer are credible and conservatively bounding.

### 5.3.2 Uncertainties in buffer erosion models

Mechanistic models of buffer erosion are complex because they must account for the chemistry, surface chemistry, physics, rheology, hydrology and transport phenomena of colloidal systems interacting with flowing groundwater. As a result, it seems likely that the models will only be applied to highly idealized systems, and, if so, this raises the question whether model predictions are conservative in the sense that they overestimate the erosion rate.

The force-balance approach developed by Neretnieks *et al.* (2009), for example, uses a DLVO-based representation of attractive and double-layer forces applied to an idealized system consisting of pure Na-montmorillonite colloids in a simple NaCl electrolyte solution. Such models are assumed to be conservative because repulsive forces favoring colloid formation should be maximized under these conditions in accordance with the Shulze-Hardy rule (Section 3). As noted in Section 4, however, there is a general consensus that although the conceptual basis of DLVO theory is substantially correct, the theory is also deficient in some important respects. This raises the question whether the claimed conservatism in force-balance models is valid when these deficiencies are taken into account.

It is also worth noting that empirical correlations may be required to calibrate buffer-erosion models in terms of the relative viscosities of bentonite sols as a function of the volume fraction of colloidal particles and the ionic composition of the aqueous phase (*e.g.*, Neretnieks *et al.*, 2009). Given the complexity of clay colloidal systems, the correlations are likely to be derived from experimental measurements of relative viscosities and particle volume fractions over a range of idealized clay types and simplified solution chemistry. It is unclear whether such correlations would be appropriate for repository conditions, however, because these conditions may lie outside the experimentally investigated range.

### 5.3.3 Geochemical constraints on sol stability

The relative stabilities of montmorillonite gels and sols can be interpreted in relation to environmental variables such as the total analytical concentrations of $Na^+$ and $Ca^{2+}$ dissolved in groundwater and bentonite porewaters. Such relations are important because conditions favoring sol stability are those for which the buffer is susceptible to erosion. Sol-gel stability relations are controlled in part by mass-action (*i.e.*, ion-exchange) constraints. Donnan equilibrium must also be invoked in order to relate the chemistry of solutions in the interlayer spaces between clay particles to the chemistry of an interconnected external reservoir represented by larger fluid-filled voids in the buffer and/or groundwater in the host rock. The nature of porosity in highly compacted clays is, however, a subject of considerable

debate in international nuclear-waste management programs (*e.g.*, Savage *et al.*, 2010). Ion-exchange models applied to such systems may moreover be rather approximate (Evans and Wennerström, 1999). These sources of conceptual uncertainty may complicate efforts to interpret environmental constraints on the stability of montmorillonite sols and gels.

### 5.3.4 Uncertainties in the characteristics of glacial meltwaters

The chemistry of glacial meltwaters has generally been considered in the context of buffer erosion only in terms of the CCC for $Ca^{2+}$ (representing divalent cations in general), or the total number of equivalents of positive charge per unit volume of solution. Glacial meltwaters are not simple electrolyte solutions, however. They are certainly dilute, but cation and anion concentrations can also be quite variable (Brown 2002). There is some evidence to suggest that such solutions would tend to promote ion-exchange reactions favoring the formation of montmorillonites having $Ca^{2+}$ as the dominant cation occupying exchange positions. This is potentially important because ion-ion correlations favoring strong attraction between clay colloidal particles, thus tending to inhibit buffer erosion, are known to be important when $Ca^{2+}$ constitutes more than 90% of the exchangeable cations (Section 4.2). Reactive transport processes controlling the chemical evolution of glacial meltwaters as they migrate from the surface toward the repository and interact with the host rock have also received little consideration in studies of buffer erosion.

## 5.4 Relative safety significance of different types of buffer erosion

The type of buffer erosion considered in the present study differs from that involving the release of bentonite particles at the buffer-groundwater interface by shear forces acting on the particles by rapidly flowing groundwater, or, in the process of "piping", by hydraulic forces acting on the buffer (and backfill) during re-saturation. It is interesting to speculate regarding the relative importance of these different types of buffer erosion with regard to potential impacts on repository safety, although each type will clearly have to be adequately dealt with separately in a safety case.

Buffer erosion associated with piping can in principle be mitigated to some extent by employing suitable deposition-hole selection criteria (*i.e.*, rejecting holes that have an unacceptable number of intersecting, water-conducting fractures) and by grouting. There is also some experimental evidence suggesting that this type of erosion tends to spontaneously decrease with time for reasons that are as yet unclear.

In comparison, dealing with the type of buffer erosion that could result from the formation and transport of clay colloids in dilute groundwaters may be more difficult. It seems likely that the safety consequences of this type of erosion will have to be assessed using models that are highly complex, possibly deficient in some theoretical respects (*e.g.*, Section 4), empirically calibrated, and largely untested by direct comparisons of model predictions with observations from experimental and natural systems.

## 5.5 Possible engineering measures to prevent buffer erosion

The possibility that buffer erosion could be avoided using engineering measures is suggested by the observation that buffer erosion cannot occur unless colloidal sols form. Montmorillonite sols are stable under two limiting conditions:

1. if the concentrations of divalent cations in the aqueous solution, particularly $Ca^{2+}$, are below the CCC, or
2. if monovalent cations, notably $Na^{+}$, occupy a significant fraction of the ion-exchange sites.

With regard to the first condition above, it has already been noted that the CCC for $Ca^{2+}$ has been determined to be approximately 1 mM. With regard to the second condition, it is interesting to note that montmorillonite sols have been observed to become unstable if the equivalent fraction of $Ca^{2+}$ on exchange sites ≥ 0.9 (*e.g.*, Birgersson *et al.*, 2009). This behavior has been attributed to the effects of ion-ion correlations, which are not accounted for in DLVO theory and which can strongly increase the net attraction between colloidal particles having high surface charge and divalent counterions in the electrical double layer (Section 4.2).

Equilibrium constraints for the ion-exchange reaction, $Ca^{2+}$(solution) + $2Na^{+}$(montmorillonite) = $2Na^{+}$(solution) + $Ca^{2+}$(montmorillonte), can be used to gain insights as to how the second condi-

tion of sol stability noted above is related to water chemistry. Mass-action constraints associated with this reaction can be represented by (Birgersson *et al.*, 2009):

$$K_{GT} = \frac{X_{Ca} a_{Na^+}^2}{X_{Na}^2 a_{Ca^{2+}}}, \quad (32)$$

where $K_{GT}$ denotes a selectivity coefficient consistent with the Gaines-Thomas convention, $X_{Ca}$ and $X_{Na}$ refer to the equivalent charge fractions of $Ca^{2+}$ and $Na^+$ occupying exchange sites on montmorillonite, and $a_{Na+}$ and $a_{Ca^{2+}}$ stand for the activities of $Na^+$ and $Ca^{2+}$, respectively. If it is assumed that $Na^+$ and $Ca^{2+}$ are the dominant exchangeable cations involved in the reaction such that $X_{Na} = 1 - X_{Ca}$, the above equation can be re-arranged to give:

$$X_{Ca} + \frac{1}{X_{Ca}} = 2 + \frac{a_{Na^+}^2}{K_{GT} a_{Ca^{2+}}}. \quad (33)$$

The selectivity coefficient, $K_{GT}$ = 4.5 (at ≈ 25°C), and is effectively independent of the density of montmorillonite-water systems (Birgersson *et al.*, 2009). Thus, for $X_{Ca} \geq 0.9$, which would tend to favor the stability of montmorillonite gels rather than sols, $a_{Na+}^2 / a_{Ca^{2+}} \leq 0.05$.

Given the above constraints, water compositions that would tend to inhibit buffer erosion as a result of gel formation are CCC ($Ca^{2+}$) ≥ 1 mM or $a_{Na+}^2 / a_{Ca^{2+}} \leq 0.05$. Neretnieks *et al.* (2009) modeled the effects of gypsum ($CaSO_4$:$2H_2O$) solubility on the concentration of $Ca^{2+}$ in buffer porewaters and concluded that $Ca^{2+}$ concentrations could not be sustained above the CCC for many conceivable and likely conditions. The possibility that $a_{Na+}^2 / a_{Ca^{2+}}$ could be buffered at levels ≤ 0.05 by mineral additives to bentonite has received little attention in comparison. Detailed analyses of possible engineering measures that could be used to buffer CCC ($Ca^{2+}$) ≥ 1 mM or $a_{Na+}^2 / a_{Ca^{2+}} \leq 0.05$ over a number of glacial cycles that are expected to occur over the next million years are unavailable.

# 6 Concluding remarks

Treatment of the issue of buffer chemical erosion in future safety cases supporting the licensing of a spent-fuel repository in Finland could rely to some extent on fundamental surface-chemical concepts governing the formation and stability of clay colloids. The present review of these concepts suggests that although prevailing theories of colloid stability (*e.g.*, DLVO) are substantially correct, they are also deficient in some important respects (see also Kruyt 1952; Missana and Adell, 2000; Boström *et al.*, 2001; Jansson 2007; Janiak *et al.*, 2008). The limitations in the theories stem from an oversimplification of the properties of real colloids, and from a failure to consider forces acting to stabilize or flocculate colloidal systems under certain environmental conditions and at small inter-particle separation distances such as will exist in highly compacted bentonite.

It is unclear whether sufficient progress can be made over the next few years to overcome these deficiencies. Experience has shown that improvements to such models generally come at the expense of an increasing number of model parameters that must be characterized experimentally, or which must be estimated. Efforts to establish defensible upper bounds on maximum colloid concentrations in repository groundwaters, as was attempted in the SR-Can safety assessment, may therefore continue to be problematic. The use of buffer materials composed mainly of Ca-smectites rather than Na-smectites as a means of enhancing the resistance of the buffer to chemical erosion is also problematic because the possibility cannot be completely ruled out that ion exchange would alter at least some of the Ca-smectite to more sodic forms, particularly over time scales of hundreds-of-thousands of years.

If this pessimistic view proves to be justified, then dealing with the issue of buffer erosion in a safety assessment context may require consideration of other features, events and processes (FEPS) that could also play an important role in the erosion process. Such FEPs may include (*e.g.*, Arthur and Zhou, 2008):

- **Buffer-groundwater interactions.** Buffer erosion will ultimately be controlled by the interaction of repository groundwaters with the buffer. A conceptual model for the formation of clay colloids resulting from these interactions must therefore account for the manner in which changes in groundwater chemistry affect the types and concentrations of counterions in the electrical double layer of clay particles. Thermodynamic models that appropriately account for Donnan and osmotic equilibria have been developed for this purpose (*e.g.*, Karnland 1997), but the models fail in some cases (*e.g.*, Ca-dominated systems) for reasons that remain unclear (Karnland 2007). The conceptual basis of the models has moreover been questioned on the grounds of whether the buffer behaves like an efficient semi-permeable membrane at high densities (*e.g.*, Dixon 2000; Bradbury and Baeyens, 2002) or whether the microstructure of the buffer needs to be taken into account (for opposing views see Muurinen *et al.*, 2004 and Birgersson and Karnland, 2009).

- **Colloid transport.** Models of buffer erosion may have to account for the transport and fate of clay colloids in the near field and geosphere. Filtering of colloids in fractures and in filter cakes composed of non-colloidal accessory minerals in a partially eroded buffer could potentially trap colloidal particles in the buffer, or reduce

groundwater flow rates in the vicinity of deposition holes (Neretnieks 2008; Martinet 2008; Richards 2008). Models of colloid formation and transport at the bentonite-groundwater interface may be complicated by differences in the rheological properties of bentonite flocs, gels and sols, especially in cases where the bentonites contain mixed Na/Ca smectites (Börgesson and Nilsson, 2008).

- **Hydrology and hydrochemistry of glacial meltwaters.** The time during which glacial meltwaters might circulate to repository depths, and the chemical characteristics of these solutions, are uncertain (Neretnieks 2007). Water-rock interactions will occur as dilute glacial meltwaters migrate toward the repository. Resultant changes in the aqueous speciation of these solutions may be such that the concentrations of "free" species (*e.g.*, $Ca^{2+}$) are sustained well below their CCC due to the formation of other species having lower valencies [*e.g.*, $CaHCO_3^+$ and/or $CaCO_3(aq)$].

It is recommended that STUK should critically evaluate these FEPs, and possibly others, to further prepare for its review of future license applications from Posiva for a KBS-3 repository in Finland.

# 7 References

Adamson AW. 1967. Physical chemistry of surfaces, 2nd ed. Interscience Publ., John Wiley & Sons, New York.

Apted M, Arthur R, Bennett D, Savage D, Sallfors G, Wennerstrom H. 2010. Buffer erosion: An overview of concepts and potential safety consequences. SSM Report 2010:31, Swedish Radiation Safety Authority, Stockholm, Sweden.

Arthur R, Zhou W. 2008. Status of research on chemical erosion of the buffer. In: Review of SKB's safety assessment SR-Can: Contributions in support of SKI's and SSI's review by external consultants. SKI Report 2008:16 (SSI Report 2008:06), Swedish Nuclear Power Inspectorate, Stockholm, Sweden.

Birgersson M. 2007. Untitled. Presented at the Workshop on Buffer Erosion (IV), June 13, 2007, Stockholm, Sweden.

Birgersson M, Karnland O. 2009. Ion equilibrium between montmorillonite interlayer space and an external solution: Consequences for diffusional transport. Geochim. Cosmochim. Acta, 73, 1908-1923.

Birgersson M, Hedström M, Karnland O, Jönsson B. 2008. Effects of ion equilibrium on sol formation of montmorillonite. Presented at the 7th workshop on bentonite erosion, December 9, 2008, Stockholm, Sweden. (www.kemi.kth.se/nuchem/be).

Birgersson M, Börgesson L, Hedström M, Karnland O, Nilsson U. 2009. Bentonite erosion. SKB TR-09-34, Swedish Nuclear Fuel and Waste Management Co., Stockholm, Sweden.

Börgesson L, Hernelind J. 2006. Consequences of loss or missing bentonite in a deposition hole: A theoretical study. SKB TR-06-13, Swedish Nuclear Fuel and Waste Management Co., Stockholm, Sweden.

Börgesson L, Sandén T. 2006. Piping and erosion in buffer and backfill materials: Current knowledge. SKB R-06-80, Swedish Nuclear Fuel and Waste Management Co., Stockholm, Sweden.

Börgesson L, Nilsson U. 2008. Erosion in fractures: Rheological properties of bentonite penetrating into fractures. Presented at the 7th workshop on bentonite erosion, December 9, 2008, Stockholm, Sweden. (www.kemi.kth.se/nuchem/be).

Boström M, Williams DRM, Ninham BW. 2001. Specific ion effects: Why DLVO theory fails for biology and colloid systems. Phys. Rev. Lett. (online), 87 (16), 168103, 4 pages.

Bradbury MH, Baeyens B. 2002. Porewater chemistry in compacted re-saturated MX-80 bentonite: Physico-chemical characterization and geochemical modelling. PSI Bericht Nr. 02-10, Paul Scherrer Institut, Villigen, Switzerland.

Brown GH. 2002. Glacial meltwater chemistry. Applied Geochemistry, 17, 855–883.

Comsol. 2004. Femlab user's guide, version 3.1. The Comsol Co., Stockholm, Sweden.

Derjaguin BV, Landau L. 1941. Theory of the stability of strongly charged lyophobic sols and of the adhesion of strongly charged particles in solutions of electrolytes. Acta Phys. Chem., 14, 633.

Dixon DA. 2000. Porewater salinity and the development of swelling pressure in bentonite-based buffer and backfill materials. Posiva Report 2000-04, Posiva Oy, Helsinki, Finland.

Evans DF, Wennerström H. 1999. The colloidal domain. Wiley VCH, New York.

Everett DH. 1971. Manual of symbols and terminology for physicochemical quantities. Appendix II: Definitions, terminology and symbols in colloid and surface chemistry (Part 1). International Union of Pure and Applied Chemistry, Division of Physical Chemistry, Washington, D.C.

García-García S, Wold S, Jonsson M. 2007. Kinetic determination of critical coagulation concentrations for sodium- and calcium-montmorillonite colloids in NaCl and $CaCl_2$ aqueous solutions. J. Colloid Interface Sci., 315, 512–519.

García-García S, Wold S, Jonsson M. 2009. Effects of temperature on the stability of colloidal montmorillonite particles at different pH and ionic strength. Appl. Clay Sci., 43, 21–26.

Grim RE. 1968. Clay mineralogy. McGraw-Hill, New York.

Hamaker HC. 1937. The London – van der Waals attraction between spherical particles. Physica, 4 (10), 1058–1072.

Hedström M, Hansen E, Karnland O, Birgersson M, Nilsson U. 2008. Colloid release from montmorillonite. Presented at the 7th workshop on bentonite erosion, December 9, 2008, Stockholm, Sweden. (www.kemi.kth.se/nuchem/be).

Helmy AK. 1998. The limited swelling of montmorillonite. J. Colloid Interface Sci., 207, 128–129.

Israelachvili JN. 1991. Intermolecular and surface forces. 2nd ed., Academic Press, New York.

Israelachvili JN, Adams GE. 1978. Measurement of forces between two mica surfaces in aqueous electrolyte solutions in the range 0–100 nm. J. Chem. Soc. Faraday Trans. 1, 74 (4), 975–1001.

Janiak J, Jönsson B, Åkesson T. 2008. Monte Carlo simulations of the swelling in bentonite clay. Presented at the Workshop on Buffer Erosion (V), January 28–29, 2008, Stockholm, Sweden. (www.kemi.kth.se/nuchem/be).

Jansson M. 2007. The DLVO theory. Presented at the Workshop on Buffer Erosion (III), March 29, 2007, Stockholm, Sweden. (www.kemi.kth.se/nuchem/be).

Jussila P. 2007. Thermomechanics of swelling unsaturated porous media. STUK-A223, Radiation and Nuclear Safety Authority, Helsinki, Finland.

Karnland O. 1997. Bentonite swelling pressure in strong NaCl solutions. Correlation between model calculation and experimentally determined data. SKB TR 97-31, Swedish Nuclear Fuel and Waste Management Co., Stockholm, Sweden.

Karnland O. 2007. Colloid workshop IV. Presented at the Workshop on Buffer Erosion (IV), June 13, 2007, Stockholm, Sweden.

Kjellander R, Marčelja S, Quirk JP. 1988. Attractive double-layer interactions between calcium clay particles. J. Colloid Interface Sci., 126 (1), 194–211.

Kruyt HR (ed.). 1952. Colloid science. Elsevier, New York.

Lagaly G. 2006. Colloid clay science. In: Handbook of clay science (F. Bergaya, B. K. G. Theng and G. Lagaly, eds.). Developments in Clay Science, vol. 1, Elsevier Ltd., New York.

Langmuir D. 1997. Aqueous environmental geochemistry. Prentice-Hall, Upper Saddle River, New Jersey.

Lifshitz EM. 1956. The theory of molecular attractive force between solids. Soviet Physics, 2 (1), 73.

Liu J, Neretnieks I. 2006. Physical and chemical stability of the bentonite buffer. SKB R-06-103, Swedish Nuclear Fuel and Waste Management Co., Stockholm, Sweden.

Lyklema J. 1991. Fundamentals of interface and colloid science. Vol. 1, Academic Press, London.

Martinet P. 2008. Conceptual model of straining of smectites by optimization of particle size distributions. Presented at the 7th workshop on bentonite erosion, December 9, 2008, Stockholm, Sweden. (www.kemi.kth.se/nuchem/be).

McBride MB. and Baveye, P. 2002. Diffuse double-layer models, long-range forces, and ordering in clay colloids. Soil Sci. Soc. Am. J., 66, 1207–1217.

Miller B, Marcos N. 2007. Process report – FEPs and scenarios for a spent fuel repository at Olkiluoto. Posiva 2007-12. Posiva Oy, Olkiluoto, Finland.

Missana T, Adell, A. 2000. On the applicability of DLVO theory to the prediction of clay colloids stability. J. Colloid Interface Sci., 230 (1), 150–156.

Missana T, Alonso U, Turrero, M. J. 2003. Generation and stability of bentonite colloids at the bentonite/granite interface of a deep geological radioactive waste repository. J. Contam. Hydrol., 61, 17–31.

Moreno L, Neretnieks I, Liu L. 2008. Bentonite expansion into seeping water. Exploratory modeling. Presented at the 7th workshop on bentonite erosion, December 9, 2008, Stockholm, Sweden. (www.kemi.kth.se/nuchem/be).

Muurinen A, Karnland O, Lehikoinen J. 2004. Ion concentration caused by an external solution into the porewater of compacted bentonite. Physics and Chemistry of the Earth, 29, 119–127.

Neretnieks I. 2007. Overview of experiments, modelling and other work underway and planned in the erosion project. Presented at the Workshop on Buffer Erosion (IV), June 13, 2007, Stockholm, Sweden.

Neretnieks I. 2008. Erosion project: Summary and findings. Presented at the 7th workshop on bentonite erosion, December 9, 2008, Stockholm, Sweden. (www.kemi.kth.se/nuchem/be).

Neretnieks I, Liu L, Moreno L. 2009. Mechanisms and models for bentonite erosion. SKB TR-09-35, Swedish Nuclear Fuel and Waste Management Co., Stockholm, Sweden.

Pegado L, Jönsson B, Wennerström HK. 2008. Ion-ion correlation attraction in a molecular solvent. J. Chem. Phys. (online), 129 (18), 184503, 11 pages.

Posiva 2006. TKS-2006 – Nuclear waste management of the Olkiluoto and Loviisa power plants: Program for research, development and technical design for 2007-2009. Posiva Oy, Olkiluoto, Finland.

Posiva 2010. TKS-2009 –Nuclear waste management at the Olkiluoto and Loviisa power plants, review of current status and future plans for 2010–2012. Posiva Report TKS-2009, Posiva Oy, Eurajoki, Finland.

Richards T. 2008. Colloid filtration experiments. Presented at the 7th workshop on bentonite erosion, December 9, 2008, Stockholm, Sweden. (www.kemi.kth.se/nuchem/be).

Savage D, Arthur R, Watson C, Wilson, J. 2010. An evaluation of models of bentonite pore water evolution. Research Report 2010:12, Swedish Radiation Safety Authority, Stockholm, Sweden.

SKB 2004. Interim process report for the safety assessment SR-Can. SKB R 04-33, Swedish Nuclear Fuel and Waste Management Co., Stockholm, Sweden.

SKB 2006. Long-term safety for KBS-3 repositories at Forsmark and Laxemar – a first evaluation: Main report of the SR-Can project. SKB TR-06-09, Swedish Nuclear Fuel and Waste Management Co., Stockholm, Sweden.

Sposito G. 1984. The surface chemistry of soils. Oxford University Press, New York, NY.

Stumm W, Morgan JJ. 1996. Aquatic chemistry, 3rd ed. Wiley Interscience, John Wiley & Sons, New York.

Swanton SW. 1995. Modelling colloid transport in groundwater; The prediction of colloid stability and retention behaviour. Adv. Colloid Interface Sci., 54, 129–208.

van Olphen JH. 1977. An introduction to clay colloid chemistry, 2nd ed., Wiley-Interscience, New York.

Verwey EJW, Overbeek JTG. 1948. Theory of the stability of lyophobic colloids. Elsevier, Amsterdam, the Netherlands.

# Part II: An evaluation of swelling pressure models for the buffer and backfill

# Contents

SUMMARY II-3

1 INTRODUCTION II-4

2 EMPIRICAL CORRELATIONS II-6

3 THERMODYNAMIC MODELS II-7
3.1 Equilibrium constraints on swelling pressure II-7
3.2 Donnan equilibria II-8
3.3 Ideal versus real Donnan systems II-9
3.4 Significance of non-ideal Donnan behavior on $p_{swell}$ II-12

4 CONCLUDING REMARKS FROM A REGULATORY PERSPECTIVE II-13

5 REFERENCES II-14

# Summary

This report considers modeling approaches that have been proposed to characterize the swelling pressure ($p_{swell}$) of buffer and backfill materials in a KBS-3 repository for spent nuclear fuel. The swelling pressure is important because many of the performance targets that are being considered for the buffer and backfill in a KBS-3 repository at Olkiluoto are defined by this parameter.

A unified mechanistic modeling approach, capable of accurately predicting the effects of material properties and environmental conditions on $p_{swell}$, is not presently available and is unlikely to become available within the foreseeable future. Alternative, thermodynamics-based modeling approaches are inherently non-mechanistic and therefore cannot account *a priori* for the effects of electrical interactions near clay surfaces on the chemical potential of water. Thermodynamics-based models that have been proposed specifically for the KBS-3 buffer are semi-empirical and are based on an assumption of ideal Donnan behavior that may not be valid. If not, interpretations of experimental observations based on these models, though possibly correct in principle, are essentially curve-fitting exercises and provide little predictive capability. The models have moreover been applied only to highly idealized systems of nominal relevance to a repository at Olkiluoto.

Given these conceptual model uncertainties, an alternative approach based on empirical correlations derived from experimental determinations of $p_{swell}$ as a function of saturated density and covering as broad a range as possible of relevant material types and environmental conditions (e.g., groundwater salinities and compositions) could help enhance confidence that performance targets for the buffer and backfill can be met. Such an approach should ideally be guided by a systematic assessment of plausible, as well as possible "outlier", environmental conditions that could exist at Olkiluoto over the assessment time period considered in a safety case.

# 1 Introduction

This study addresses approaches that have been proposed to characterize the swelling pressure ($p_{swell}$) of buffer and backfill materials in a KBS-3 repository for spent nuclear fuel. In this context, $p_{swell}$ is defined as the mechanical force per unit area exerted by the swelling-clay component of bentonite (montmorillonite) on confinement structures represented by deposition holes (buffer) or deposition tunnels (backfill).

The swelling pressure is important in relation to repository safety because many of the performance targets for the buffer and backfill are defined by this parameter. Figure 1, for example, illustrates how swelling pressures in the buffer might vary as a function of saturated density, and how these variations would relate to several performance targets, including the prevention of significant microbial activity ($p_{swell}$ > 2 MPa); the provision of sufficient tightness and self-sealing ability ($p_{swell}$ > 1 MPa); and the prevention of canister sinking ($p_{swell}$ > 0.1 MPa). Also, because swelling pressure and hydraulic conductivity are closely related, a performance target to prevent significant advective transport can be stated in terms of hydraulic conductivity (K < $10^{-12}$ m $s^{-1}$) (Posiva 2010) or swelling pressure ($p_{swell}$ > 0.1 MPa) (SKB 2006a). Similarly for the backfill, a performance target of K < $10^{-10}$ m $s^{-1}$ corresponds to $p_{swell}$ > 0.2 MPa for an assumed groundwater salinity of 35 g $l^{-1}$ (Pastina and Hellä, 2006).

Two general mechanisms control the swelling behavior of clay minerals (*e.g.*, Madsen and Müller-VonMoos, 1989):

- innercrystalline swelling, which results from the uptake of water to hydrate clay surfaces and exchangeable cations, and
- osmotic swelling, which results from concentration differences involving ions associated with clay surfaces and those in an external solution.

Innercrystalline swelling is controlled by the layer charge of the clay mineral and hydration properties of the interlayer cations. It is generated in a stepwise manner with development of up to 4 monolayers of water. Osmotic swelling operates over larger distances and is controlled by the negatively charged clay surface and a diffuse electrical double of charge that extends into the adjacent aqueous phase. As two clay particles closely approach one another a repulsive force per unit area develops between them that depends on the excess concentration, relative to the bulk porewater, of cations in the overlapping double layers at a location midway between the particles.

Several types of models have been proposed to account for physical and chemical processes controlling the swelling pressure of compacted clays (Karnland 1998; Dixon 2000; Savage 2005; Agus and Schanz, 2008). Empirical models, which attempt to relate $p_{swell}$ to the interlamellar distance between individual clay particles (Low 1979; 1980), are simple and utilitarian, but model parameters must be calibrated experimentally and results are not always easy to obtain or physically meaningful (Grauer 1986). Diffuse double-layer (DDL) models, which attempt to relate $p_{swell}$ to repulsive interactions arising from the overlap of electrical double layers associated with the charged surfaces of clay particles [*e.g.*, Yong *et al.*, 1992; Komine and Ogata, 1994; 1996 (see also Sridharan 1997)], are based on well-established theoretical concepts for colloidal systems (*e.g.*, Kruyt 1952; Adamson 1967), but are difficult to apply to highly compacted clays due in part to structural modifications of water that occur in the interlamellar regions of clay particles (*e.g.*, Low 1987).

Because of these difficulties it has been concluded that although discussions regarding the mechanisms involved in controlling $p_{swell}$ in compacted clays have been ongoing for decades, it is unlikely

that a unified mechanistic modeling approach will emerge from these discussions within the foreseeable future (Dixon 2000). Pastina and Hellä (2006) refer to Karnland and Birgersson (2006) in similarly concluding that there is no general consensus concerning detailed mechanisms controlling the swelling pressure, or in models that can be used to calculate $p_{swell}$ as a function of material properties or environmental parameters.

Assuming this is true, the question arises as to whether confidence is warranted in claims that $p_{swell}$ in the buffer and backfill will be sufficient to ensure that the respective performance targets will be met over the entire assessment time period considered in a safety case. The present report considers two approaches that have been proposed to answer this question: 1) the development of empirical correlations between $p_{swell}$, material properties and environmental conditions (notably groundwater salinities) based on experimental observations, and 2) the application of non-mechanistic, thermodynamics-based models to predict $p_{swell}$ as a function of these properties and conditions.

The empirical approach is considered further below (Section 2). This is followed by an evaluation of thermodynamic models relevant to the KBS-3 disposal concept (Section 3). The advantages and limitations of these two approaches are considered from a safety-assessment perspective in Section 4.

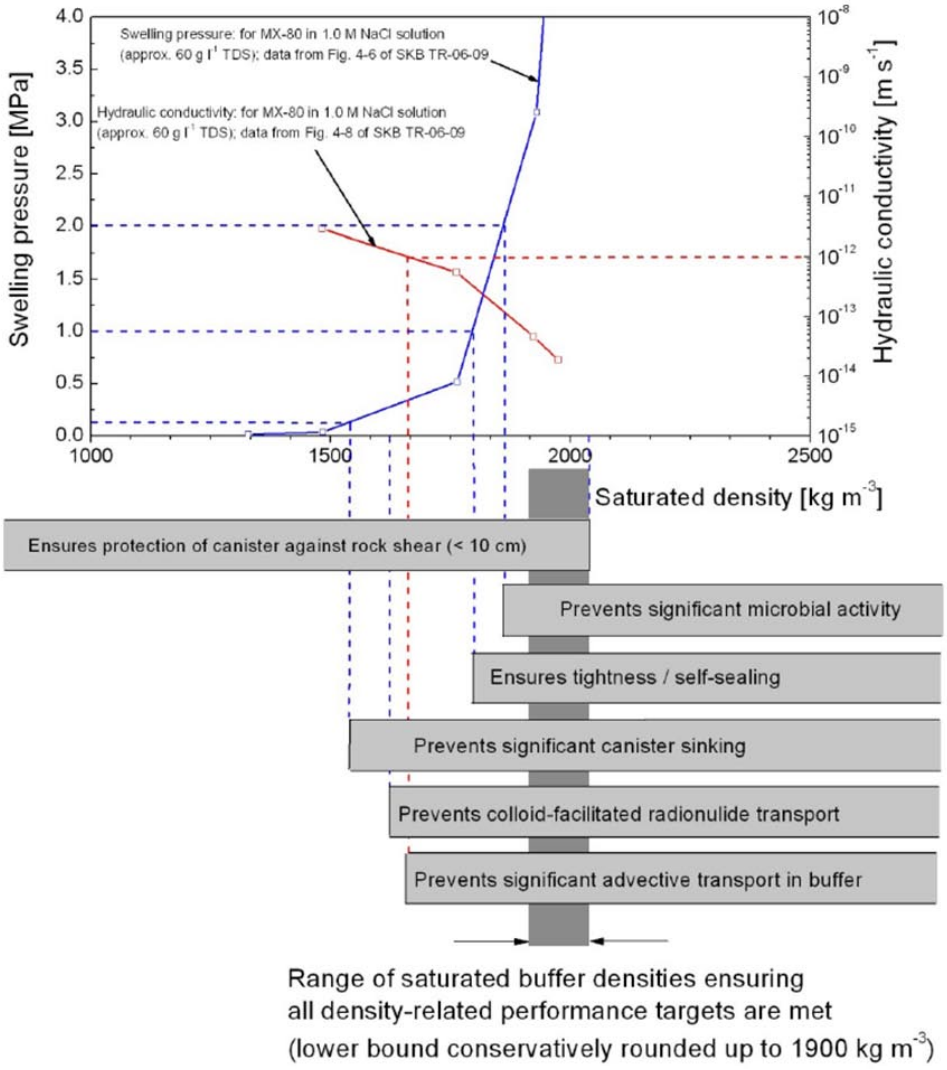


**Figure 1.** Schematic illustration of the effects of buffer saturated density on the swelling pressure, hydraulic conductivity, and related performance targets (Posiva 2010).

# 2 Empirical correlations

Dixon (2000) questioned whether reliable swelling pressure models for the buffer and backfill can be developed in a timely manner for reasons stated in the preceding section, and proposed that a database of experimental measurements could instead be constructed and used to establish empirical correlations between $p_{swell}$ and density. An example is shown in Figure 2, where swelling pressures determined in tests involving various bentonites and aqueous solutions are plotted as a function of the "effective clay dry density" (ECDD = dry mass of clay divided by the volume occupied by the clay plus the void volume[1]). The lines in the figure represent the results of regression analyses for tests involving fresh water, brackish water, saline water and brine. Dixon (2000) noted that the regression lines are similar, indicating little influence of salt on the swelling behavior as long as the ECDD is above about 0.9 Mg $m^{-3}$, but that the limited number of available measurements at high salt concentrations generates significant uncertainty in the regression results. Agus and Schanz (2008) have developed similar correlations for bentonite-sand mixtures.

A similar empirical approach could conceivably be applied to specific conditions expected in a KBS-3 repository at Olkiluoto. Uncertainties in regression correlations between $p_{swell}$ and density may be minimized if the experimental measurements were limited to specific buffer and backfill compositions planned for use in the repository. Correlations could be developed from the results of experimental investigations of the swelling properties of candidate buffer and backfill materials planned by Posiva (Posiva 2010).

Dixon (2000) considered variations in environmental conditions only in terms of a range of groundwater salinities. In studies of the effects of salt solutions on swelling pressure, however, Herbert and Moog (1999; 2000) and Herbert *et al.* (2004) have shown that other aspects of solution chemistry can strongly affect swelling pressure. For example, Herbert and Moog (2000) found that in tests involving MX-80 bentonite and saturated NaCl solutions $p_{swell}$ increased with increasing Mg content if the K concentration was held constant, and that K played the dominant role in affecting $p_{swell}$ in a series of tests in which both Mg and K varied.

If solution chemistry rather than salinity alone can significantly affect the swelling pressure of the buffer and backfill, then it would seem reasonable to expect that an empirical approach such as that described by Dixon (2000) should ideally be guided by a systematic assessment of plausible, as well as possible "outlier", environmental conditions. Plausible bounds on groundwater salinities in the vicinity of Olkiluoto over the assessment time period considered in a safety case have been established by Posiva (*e.g.*, Pastina and Hellä, 2006), but, to the author's knowledge, similar bounds on other solution constituents, such as $K^+$ and $Mg^{2+}$, which could affect the swelling pressure have not been determined.

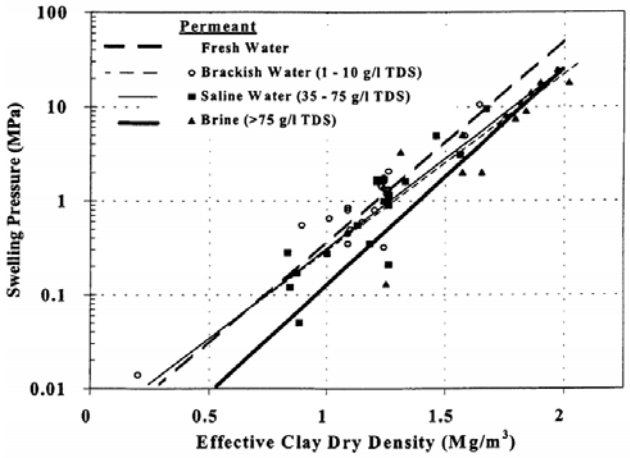


**Figure 2.** Empirical correlations between experimental measurements of pswell and effective clay dry density (Dixon 2000).

1 Dixon (2000) noted that the ECDD for the Finnish KBS-3 reference buffer is 1.6 Mg $m^{-3}$

# 3 Thermodynamic models

Non-mechanistic, thermodynamics-based models have been used to interpret the results of experimental investigations of the swelling properties of buffer materials that could be used in a KBS-3 repository in Finland or Sweden (Karnland 1998; Muurinen *et al.*, 2004; Karnland *et al.*, 2005; Birgersson *et al.*, 2008; Agus and Schanz, 2008; Birgersson and Karnland, 2009). Figure 3 illustrates the conceptual basis of such models. One region of the model domain consists of an aqueous phase and clay minerals (representing the buffer or backfill) and the other region contains only an aqueous solution at the same temperature (representing groundwater in the near-field rock). The clay minerals are assumed to have a net negative layer charge resulting from isomorphous substitutions of cations in octahedral and tetrahedral sites. The boundary between the two model domains is assumed to be permeable with respect to aqueous solutes and water, but not with respect to the clay minerals.

A simplified version of this conceptual model was considered in the modeling studies noted above. Aqueous solutions in both model domains were assumed to be simple NaCl solutions. All clay minerals were assumed to have the same layer charge, and $Na^+$ was assumed to be the only exchangeable cation. Equilibrium constraints consistent with this simplified conceptual model are discussed below.

## 3.1 Equilibrium constraints on swelling pressure

The chemical potential of water ($\mu_w$) in the "rock" region of Figure 3 is given by:

$$\mu_w = \mu_w^o + RTlna_w + \overline{v}_w p \qquad (1)$$

where $\mu_w^o$ refers to standard-state conditions, $R$ stands for the gas constant, $T$ denotes temperature, $a$ represents activity, $\overline{v}$ refers to molar volume and $p$ stands for pressure. In the "clay" region:

$$\mu'_w = \mu_w^o + RTlna'_w + \overline{v}_w p' \qquad (2)$$

(accented symbols here and in the following discussion refer to the clay region). Because water can pass freely through the boundary separating the two regions, its chemical potential must be the same in both regions at equilibrium. Equating Equations. (1) and (2) and rearranging:

$$p' - p = -\frac{RT}{\overline{v}_w} ln\left(\frac{a'_w}{a_w}\right), \qquad (3)$$

where the pressure difference represents the swelling pressure.

Noting that $a_w \equiv p_w / p_w^o$ and $a'_w \equiv p'_w / p_w^o$, where $p_w$, $p'_w$ and $p_w^o$ represent vapor pressure in the rock region, clay region and standard state, respectively (vapor pressure and fugacity are assumed to be equal), Equation (3) can be rearranged

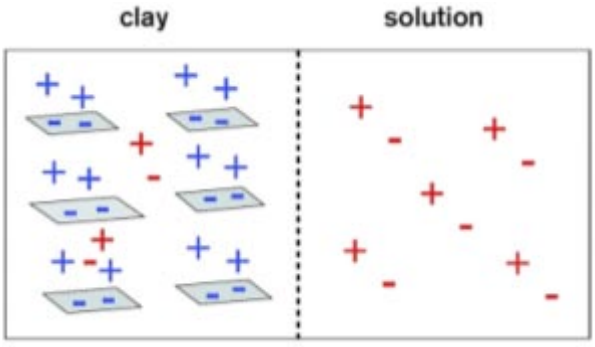


**Figure 3.** Schematic diagram of a swelling-pressure model for the buffer and backfill (SKB 2006b). The left side of the diagram represents the clay buffer (or backfill), and contains negatively charged clay particles (gray sheets with exchangeable cations indicated by blue crosses) and an aqueous NaCl solution (red symbols). The right side of the diagram represents the near-field rock, and contains an aqueous NaCl solution in pores. The boundary between the two regions (dashed line) is assumed to be permeable to $Na^+$, $Cl^-$ and water, but impermeable to clay particles.

to give:

$$p' - p = p_{\text{swell}} = -\frac{RT}{\overline{v}_w}\left( ln\frac{p'_w}{p^o_w} - ln\frac{p_w}{p^o_w} \right). \quad (4)$$

Karnland (1998) noted that water in the clay region would be affected both by interactions with the negatively charged clay particles and by interactions with the electrolyte. To distinguish the effects of these interactions on $p_{swell}$, Equation (4) was expanded to:

$$p_{\text{swell}} = -\frac{RT}{\overline{v}_w}\left( ln\frac{p'_{w,c}}{p^o_w} + ln\frac{p'_{w,ie}}{p^o_w} - ln\frac{p_w}{p^o_w} \right), \quad (5)$$

where, following Karnland's notation, the first term inside the bracket refers to water impacted by interactions with the clay and the second term represents the effects of interactions involving the "introduced" electrolyte. The contribution of the first term to $p_{swell}$ can be determined experimentally if the electrolyte concentration is sufficiently low that to a good approximation $p_w / p^o_w = p'_{w,ie} / p^o_w = 1$. It is worth noting that the thermodynamic model does not provide a basis for predicting the effects of this term on $p_{swell}$ *a priori*.

Karnland related the second and third terms on the right-hand side of Equation (5) to the osmotic pressure (π) in the clay and rock domains, respectively. The osmotic pressure is given by (*e.g.*, Denbigh 1978):

$$\pi = RT\sum \rho m_j = -\frac{RT}{\overline{v}_w} ln a_w, \quad (6)$$

where ρ stands for the density of the aqueous phase and $m_j$ represents the molality of the $j$-th solute (*e.g.*, if electrolyte NaCl dissociates completely, $j$ refers to the ions $Na^+$ and $Cl^-$)[2]. Substituting this relation for the second and third terms on the right-hand side of Equation (5) results in:

$$p_{\text{swell}} = -\frac{RT}{\overline{v}_w} ln\frac{p'_{w,c}}{p^o_w} - RT\left(\sum \rho m_j - \sum \rho' m'_j\right). \quad (7)$$

Karnland (1998) derived a similar expression in terms of electrolyte concentration using a van't Hoff factor to account for the extent of electrolyte dissociation (which was apparently assumed to be the same in both the rock and clay domains). Equilibrium constraints on the last two terms on the right-hand side of Equation (7) are considered in the following section.

## 3.2 Donnan equilibria

The effects of ion concentration on $p_{swell}$ can be interpreted in relation to the Donnan equilibrium (Karnland 1998; Karnland *et al.*, 2005). A simplified Donnan system representing conditions in the buffer (or backfill) and immediately surrounding host rock is shown in Figure 3. As noted earlier, the system consists of a compacted Na-clay separated from an external NaCl solution by a membrane permeable to $Na^+$ and $Cl^-$ but not to individual clay particles. Corresponding equilibrium constraints on $Na^+$ and $Cl^-$ concentrations in the clay porewater and external solution are derived below (Davis 1942; Marshall 1948; Hanshaw and Coplen, 1973).

Diffusion of $Na^+$ and $Cl^-$ through the membrane will occur until the net movement of these ions ceases and equilibrium is reached. The chemical potential of the salt in the clay porewater and external solution will then be equal:

$$\mu_{\text{NaCl}} = \mu'_{\text{NaCl}}. \quad (8)$$

The chemical potentials for the electrolyte are related to individual ion activities by:

$$\mu_{\text{NaCl}} = \mu^o_{\text{NaCl}} + RTln(a_{\text{Na}^+} a_{\text{Cl}^-}) \quad (9)$$

$$\mu'_{\text{NaCl}} = \mu'^o_{\text{NaCl}} + RTln(a'_{\text{Na}^+} a'_{\text{Cl}^-}) \quad (10)$$

where $\mu^o_{\text{NaCl}}$ and $\mu'^o_{\text{NaCl}}$ refer to conditions in the standard state. Assuming these conditions are the same for clay porewater and the external solution, Equations (8) – (10) can be combined to give:

$$a_{\text{Na}^+} a_{\text{Cl}^-} = a'_{\text{Na}^+} a'_{\text{Cl}^-}. \quad (11)$$

Equality of the product of the activities of an electrolyte's ions in different regions of a Donnan system defines the Donnan equilibrium.

Evaluation of Equation (7) requires that the concentrations of ions in different regions of a Donnan system be known. A suitable relation among these concentrations can be derived using electrical neutrality constraints. Continuing with the model system discussed above, for example:

$$m'_{\text{Na}^+} = m'_{\text{Cl}^-} + n'_{\text{A}}, \quad (12)$$

where $n'_{\text{A}}$ represents the number of equivalents of negative charge (equal to the number of equivalents of exchangeable $Na^+$) associated with clay minerals

2 Note that the units for $R$ in this equation must be compatible with those of the product $\rho m_j$ (mol $l^{-1}$).

per 1000 g of water. Noting that $a_i \equiv \gamma_i m_i$ ($\gamma_i$ stands for the activity coefficient of the $i$-th aqueous species), Equation (12) can be rewritten:

$$\frac{a'_{Na^+}}{\gamma'_{Na^+}} = \frac{a'_{Cl^-}}{\gamma'_{Cl^-}} + n'_A \quad . \tag{13}$$

Substituting Equation (11) into Equation (13) results in:

$$\frac{a'_{Na^+}}{\gamma'_{Na^+}} = \frac{a_{Na^+} a_{Cl^-}}{a'_{Na^+}\gamma'_{Cl^-}} + n'_A . \tag{14}$$

Then, multiplying by $a'_{Na^+} / \gamma'_{Na^+}$ and rearranging:

$$\left(\frac{a'_{Na^+}}{\gamma'_{Na^+}}\right)^2 - \frac{a_{Na^+} a_{Cl^-}}{\gamma'_{Na^+}\gamma'_{Cl^-}} - n'_A \frac{a'_{Na^+}}{\gamma'_{Na^+}} = 0. \tag{15}$$

Solving this quadratic equation results in:

$$\frac{a'_{Na^+}}{\gamma'_{Na^+}} = \frac{n'_A}{2} + \sqrt{\frac{n'^2_A}{4} + \frac{a_{Na^+} a_{Cl^-}}{\gamma'_{Na^+}\gamma'_{Cl^-}}}, \tag{16}$$

or,

$$m'_{Na^+} = \frac{n'_A}{2} + \sqrt{\frac{n'^2_A}{4} + \frac{a^2_\pm}{\gamma'^2_\pm}} \ , \tag{17}$$

where $a_\pm$ and $\gamma_\pm$ represent the mean activity and mean activity coefficient, respectively [$a_\pm \equiv (a_+ a_-)^{1/2}$ and $\gamma_\pm \equiv (\gamma_+ \gamma_-)^{1/2}$] (the negative root of Eqn. (15) is not meaningful because it gives negative values of $m'_{Na^+}$). Similar reasoning results in the following expression for $Cl^-$:

$$m'_{Cl^-} = -\frac{n'_A}{2} + \sqrt{\frac{n'^2_A}{4} + \frac{a^2_\pm}{\gamma'^2_\pm}} \ , \tag{18}$$

and, combining this result with Equation (17)

$$m'_{Na^+} + m'_{Cl^-} = 2\sqrt{\frac{n'^2_A}{4} + \frac{a^2_\pm}{\gamma'^2_\pm}}. \tag{19}$$

This sum controls $p_{swell}$ because it constrains the third term on the right-hand side of Equation (7).

In a similar derivation, Karnland (1998) assumed $\gamma'^2_\pm = \gamma^2_\pm$. With this assumption Equation (16) becomes:

$$\frac{a'_{Na^+}}{\gamma'_{Na^+}} = \frac{n'_A}{2} + \sqrt{\frac{n'^2_A}{4} + \frac{a_{Na^+} a_{Cl^-}}{\gamma_{Na^+}\gamma_{Cl^-}}} = \frac{n'_A}{2} + \sqrt{\frac{n'^2_A}{4} + m_{Na^+} m_{Cl^-}} \ , \tag{20}$$

and, because in the external solution charge balance requires $m_{Na+} = m_{Cl-}$,

$$\frac{a'_{Na^+}}{\gamma'_{Na^+}} = m'_{Na^+} = \frac{n'_A}{2} + \sqrt{\frac{n'^2_A}{4} + m^2_{Na^+}} \quad . \tag{21}$$

This equation was used by Karnland (1998) and Karnland *et al.* (2005) to calculate ionic contributions to $p_{swell}$.

## 3.3 Ideal versus real Donnan systems

An ideal Donnan system is one for which $\gamma^2_\pm = \gamma'^2_\pm$ (Davis 1942)[3]. Under such conditions, Equation (11) becomes:

$$m_{Na^+} m_{Cl^-} = m'_{Na^+} m'_{Cl^-}. \tag{22}$$

Ideal behavior has generally been assumed in studies of Donnan equilibria involving clay materials due to experimental difficulties in determining the ionic compositions of clay porewaters (*e.g.*, Davis 1942; Hanshaw and Coplen, 1973; Leroy *et al.*, 2007). Ideal behavior was assumed in experimental and modeling studies of Donnan equilibria related specifically to the KBS-3 buffer and backfill (Karnland 1998; Karnland *et al.*, 2005; Birgersson and Karnland, 2009).

An experimental study by Muurinen (2006) (see also Muurinen *et al.*, 2004) of porewater chemistry in samples of compacted MX-80 bentonite used in the swelling-pressure tests of Karnland *et al.* (2005) provides a basis for evaluating whether this assumption is valid. The experimental apparatus used in the swelling-pressure tests is shown in Figure 4. Samples of purified MX-80 bentonite in which montmorillonite had been exchanged to the sodium form were compacted and placed in the cylindrical sample holder. The piston, pressure transducer and upper lid were attached and a NaCl solution was then slowly circulated behind the bottom filter. At full saturation the bentonite

3 It is not necessary that the aqueous phases in different regions of a Donnan system must themselves be ideal.

sample was isolated from the circulating solution by the filter, which, although impermeable to the transport of clay particles, allowed for the exchange of $Na^+$ and $Cl^-$ between the bentonite porewater and external solution. Tests were terminated after pressure equilibrium had been achieved and a minimum test period of 1 month had elapsed. The bentonite sample and circulating solution were then removed from the test apparatus and characterized.

Muurinen (2006) sampled porewaters in the bentonite samples by squeezing the samples under an applied load. The sampling system consisted of a pressing apparatus to create long-term compression and a compaction cell. Porewaters were separated from bentonite in the compaction cell using a steel sinter, and the separated solutions were collected in a syringe.

Pressure was applied to the sample in a step-wise manner up to 100 MPa. In some cases several porewater samples were obtained from a given bentonite sample over a range of step-wise increases in pressure. All porewaters and external solutions were ultra-filtered and analyzed for total dissolved Na, Cl, Total Dissolved Solids (TDS), and, in some cases, Ca, Mg, Si, $SO_4$ and $HCO_3$.

Table 1 summarizes the analytical data for Na and Cl. Sample numbers are those of Muurinen *et al.* (2006). Multiple porewater samples squeezed from a given bentonite sample over a range of increasing pressures are indicated by numbers following the "/" symbol (the progression 1, 2, 3,

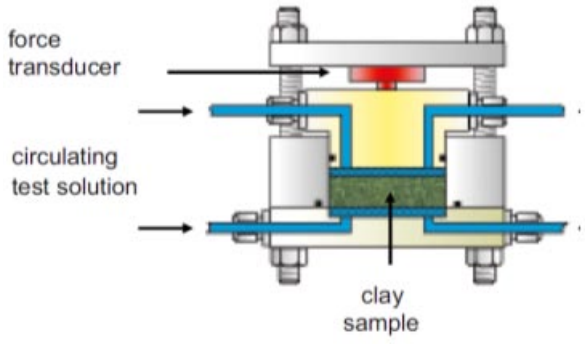


**Figure 4.** Schematic diagram of the sample holder used in swelling-pressure tests carried out by Karnland et al. (2005). Circulating solutions passed only through the bottom circuit in these tests (i.e., not through the upper circuit as indicated in the figure). The filter allowed water and aqueous solutes to pass between the clay sample and circulating solution, but not clay particles.

etc., corresponds to increasing applied load). The original analytical data, reported in mg $l^{-1}$, were converted to molalities in the present study using solution densities calculated using the Geochemist's Workbench geochemical modeling software package (Bethke 2008). Significant charge imbalances (up to about +12%) were calculated in some cases when the analyses included only $Na^+$ and $Cl^-$.

The analytical data in Table 1 were used to assess whether the swelling-pressure results of Karnland *et al.* (2005) are consistent with ideal Donnan behavior as represented by Equation (22). The data in this table refer to total dissolved concentrations. For Na, the total concentration represents the sum of concentrations of the free cation, $Na^+$, plus that of the ion-pair NaCl(*aq*) (other $Na^+$ ion pairs are unlikely to be important given the experimental conditions). For Cl, the total concentration represents the sum of concentrations of the free anion, $Cl^-$, plus NaCl(*aq*). It is reasonable to assume that the NaCl(*aq*) content of the external circulating solutions used in the experiments was negligible compared to that of $Na^+$ and $Cl^-$ given the limited extent to which this ion pair forms in bulk aqueous solutions at room temperature (Pokrovskii and Helgeson, 1995)[4]. The molalities of the free cation and anion in these solutions are therefore given to a good approximation by the respective total molalities.

It is unclear whether this assumption is also reasonable for bentonite porewaters, however. The electrical properties of montmorillonite surfaces are likely to influence the dielectric properties of nearby $H_2O(l)$, for example, and this could favor formation of NaCl(*aq*) at the expense of $Na^+$ and $Cl^-$. As a first approximation it was therefore assumed as a limiting case that porewater $Na^+$ and $Cl^-$ concentrations are given by their respective analytical concentrations. The effects of ion-pairing were then considered qualitatively in relation to this assumption.

The results in Table 1 indicate that the product of $Na^+$ and $Cl^-$ molalities in external solutions are not equal to their counterparts in bentonite porewaters, suggesting that the experimental system used in the swelling-pressure tests was not an ideal

4 For a 1 molal NaCl solution at 25°C, for example, NaCl(*aq*) would amount to just 6% of the total analytical concentration of Na and Cl.

**Table 1.** Analytical data for Na and Cl in external solutions and MX-80 porewaters (Muurinen 2006). Corresponding $m_{Na+}m_{Cl-}$ values were calculated in the present study.

| Sample Number | External Solution | | | Porewater | | |
|---|---|---|---|---|---|---|
| | $Na^+$ (mg $l^{-1}$) | $Cl^-$ (mg $l^{-1}$) | $m_{Na+}m_{Cl-}$ | $Na^+$ (mg $l^{-1}$) | $Cl^-$ (mg $l^{-1}$) | $m_{Na+}m_{Cl-}$ |
| S2-2A/1 | 2930 | 4000 | 0.0139 | 2110 | 2600 | 0.0065 |
| S2-2A/2 | 2930 | 4000 | 0.0139 | 1770 | 2120 | 0.0045 |
| S2-2A/3 | 2930 | 4000 | 0.0139 | 1250 | 1510 | 0.0023 |
| S2-4A/1 | 2530 | 3870 | 0.0116 | 762 | 1014 | 0.0009 |
| S2-4A/2 | 2530 | 3870 | 0.0116 | 543 | 746 | 0.0005 |
| S2-4A/3 | 2530 | 3870 | 0.0116 | 436 | 624 | 0.0003 |
| S2-4A/4 | 2530 | 3870 | 0.0116 | 496 | 589 | 0.0004 |
| S2-5A/1 | 27600 | 37500 | 1.17 | 20600 | 29900 | 0.70 |
| S2-5A/2 | 27600 | 37500 | 1.17 | 13300 | 19400 | 0.30 |
| S2-6A/1 | 75200 | 104400 | 8.00 | 67200 | 88800 | 6.22 |
| S2-6A/2 | 75200 | 104400 | 8.00 | 46900 | 65800 | 3.35 |
| S2-8A | 28000 | 37900 | 1.20 | 13900 | 20100 | 0.32 |
| S2-9A | 75600 | 103300 | 7.96 | 50200 | 69800 | 3.77 |
| S2-11A | 23546 | 38567 | 1.03 | 9600 | 14400 | 0.16 |
| S2-12A | 74800 | 102400 | 7.82 | 48800 | 68700 | 3.62 |
| S2-13A/1 | 7400 | 10646 | 0.093 | 6458 | 9785 | 0.075 |
| S2-13A/2 | 7400 | 10646 | 0.093 | 5783 | 8625 | 0.059 |
| S2-13A/3 | 7400 | 10646 | 0.093 | 4107 | 6063 | 0.030 |
| S2-14A/1 | 7400 | 10621 | 0.093 | 3824 | 5589 | 0.025 |
| S2-14A/2 | 7400 | 10621 | 0.093 | 2779 | 3468 | 0.011 |
| S2-15A | 7400 | 10774 | 0.094 | 1960 | 2842 | 0.007 |
| S2-16A | 7400 | 11792 | 0.103 | 2247 | 3420 | 0.009 |
| S2-17A | 2592 | 4224 | 0.013 | 574 | 829 | 0.0006 |
| S2-18A | 2684 | 4409 | 0.014 | 979 | 1544 | 0.002 |

Donnan system. Figure 5 shows that ideal behavior is more closely approached as the NaCl content of the circulating solutions increases, but was not attained even in tests with 3 molal NaCl. The possible formation of NaCl($aq$) ion pairs in the bentonite porewaters would only decrease the molalities of free $Na^+$ and $Cl^-$, thus increasing differences in the product, $m_{Na+}m_{Cl-}$, between these solutions and the external solutions. Although interpretations of the swelling-pressure results based on possible effects of ion-pair formation on the van't Hoff equation (Karnland 1998; Karnland *et al.*, 2005), or on the pore structure of compacted bentonite (Muurinen 2006), may be correct in principle, such interpretations do not seem justified because they are based on an assumption of ideal Donnan behavior (*i.e.*, $\gamma_{\pm}^2 = \gamma_{\pm}'^2$) that appears to be incorrect. The experimental results are compatible with other

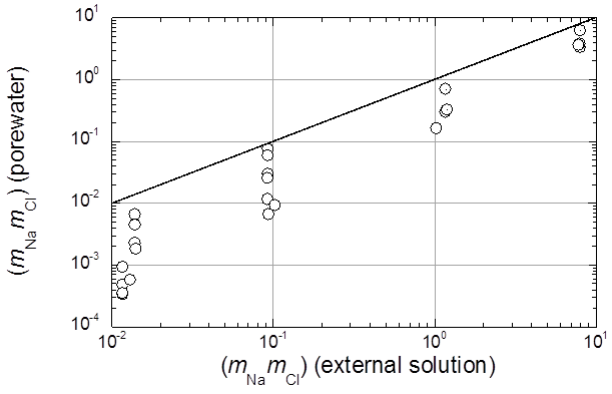


**Figure 5.** Comparison of calculated $m_{Na}m_{Cl}$ values for external solutions and squeezed porewaters based on analytical data from Muurinen (2006) for swelling-pressure tests described by Karnland et al. (2005). The line represents agreement among $m_{Na}m_{Cl}$ values for porewaters and external solutions, and is a condition for ideal Donnan behavior.

experimental studies suggesting that compacted clays are real, not ideal, Donnan systems (*e.g.*, Davis 1942; Hanshaw and Coplen, 1973).

## 3.4 Significance of non-ideal Donnan behavior on $p_{swell}$

Non-ideal Donnan behavior, such as appears to be indicated in the previous discussion by the observation $m_{Na^+} m_{Cl^-} > m'_{Na^+} m'_{Cl^-}$, would require $\gamma_{\pm}^2 < \gamma'^2_{\pm}$ to satisfy the requirement in Equation (11). The corresponding value of $m'_{Na^+}$ plus $m'_{Cl^-}$ [Eqn. (19)] would be smaller than if ideal Donnan behavior were assumed. The swelling pressure calculated using Equation (7) would therefore be lower in a real Donnan system than in its ideal counterpart if all other factors were the same in both systems. An assumption of ideal Donnan behavior, in addition to simplifying models of compacted clay systems, may therefore be conservative from a performance assessment perspective because it leads to predictions of $p_{swell}$ that are smaller than might actually occur.

# 4 Concluding remarks from a regulatory perspective

Experimental tests indicate that swelling pressures sufficient to meet performance targets for the buffer and backfill in a KBS-3 repository at Olkiluoto can be achieved. Swelling pressures at the high saturated densities envisaged for the buffer will be controlled mainly by innercrystalline swelling. Electrolyte (*i.e.*, Donnan) effects on $p_{swell}$ are expected to be relatively small at these saturated densities, but could become important if the density were to be lowered by processes such as buffer erosion. Donnan effects could also be important for the relatively low density backfill.

There appears to be a scientific consensus that a unified mechanistic modeling approach, capable of accurately predicting the effects of material properties and environmental conditions on $p_{swell}$, is not presently available and is unlikely to become available within the foreseeable future. Such mechanistic models include those that attempt to relate $p_{swell}$ to the interlamellar distance between individual clay particles, and those that attempt to relate $p_{swell}$ to repulsive interactions arising from the overlap of electrical double layers associated with the charged surfaces of clay particles. Laird (1996) and Skipper *et al.* (2006) describe recent advances in modeling innercrystalline swelling in clay-based materials.

Alternative, thermodynamics-based modeling approaches are inherently non-mechanistic and therefore cannot account *a priori* for the effects of electrical interactions near clay surfaces on the activity and chemical potential of the solvent, $H_2O(l)$. These interactions must therefore be characterized experimentally, or by adopting extra-thermodynamic assumptions and models (*e.g.*, as in DLVO theory). Thermodynamic models can, however, be combined with experimental constraints to evaluate electrolyte contributions to $p_{swell}$ consistent with the Donnan equilibrium. Such combined models are semi-empirical.

Thermodynamics-based models that have been proposed for the KBS-3 buffer are based on an assumption of ideal Donnan behavior that may be invalid. If so, interpretations of experimental observations based on these models, though possibly correct in principle, are essentially curve-fitting exercises and provide little predictive capability. The models have moreover been applied only to highly idealized systems of nominal relevance to a repository at Olkiluoto, especially over the assessment period, and associated variations in environmental conditions, that must be considered in a safety case.

If mechanistic- and thermodynamics-based modeling approaches prove to be inadequate, an empirical approach based on experimental determinations of $p_{swell}$ as a function of saturated density covering as broad a range as possible of relevant material types and environmental conditions (*e.g.*, groundwater salinities and compositions) may be needed to enhance confidence that performance targets for the buffer and backfill can be met. Such an approach should ideally be guided by an experimental program that is based on a systematic assessment of plausible, as well as possible "outlier", environmental conditions that could exist at Olkiluoto over the assessment time period considered in the safety case.

# 5 References

Adamson AW. 1967. Physical chemistry of surfaces, 2nd ed. Interscience Publ., John Wiley & Sons, New York.

Agus SS, Schanz T. 2008. A method for predicting swelling pressure of compacted bentonites. Acta Geotechnica, 3, 125–137.

Bethke C M. 2008. Geochemical and biogeochemical reaction modeling. Cambridge Univ. Press, Cambridge, U.K.

Birgersson M, Karnland O. 2009. Ion equilibrium between montmorillonite interlayer space and an external solution – Consequences for diffusional transport. Geochimica Cosmochimica Acta, 73, 1908–1923.

Birgersson M, Karnland O, Nilsson U. 2008. Freezing in bentonite – a thermodynamic approach. Physics and Chemistry of the Earth, 33, S527–S530.

Davis LE. 1942. Significance of Donnan equilibria for soil colloidal systems. Soil Science, 54 (3), 199–219.

Denbigh K. 1978. The principles of chemical equilibrium, 3rd edition. Cambridge Univ. Press, Cambridge, UK.

Dixon DA. 2000. Porewater salinity and the development of swelling pressure in bentonite-based buffer and backfill materials. Posiva 2000-04, Posiva Oy, Helsinki, Finland.

Grauer R. 1986. Bentonite as a backfill material in the high-level waste repository: Chemical aspects. Nagra Technical Report 86-12E, Nagra, Baden, Switzerland.

Hanshaw BB, Coplen TB. 1973. Ultrafiltration by a compacted clay membrane – II. Sodium ion exclusion at various ionic strengths. Geochimica Cosmochimica Acta, 37, 2311–2327.

Herbert H-J, Moog HC. 1999. Cation exchange, interlayer spacing, and water content of MX-80 bentonite in high molar saline solutions. Engineering Geology, 54, 55–65.

Herbert H-J, Moog HC. 2000. Modeling of saturation and swelling effects in clays under different saline conditions. In: Eurosafe, Cologne, Germany.

Herbert H-J Kasbohm J, Moog HC, Henning KH. 2004. Long-term behavior of the Wyoming bentonite MX-80 in high saline solutions. Applied Clay Science, 26, 275–291.

Karnland O. 1998. Bentonite swelling pressure in strong NaCl solutions. Posiva 98-01, Posiva Oy, Helsinki, Finland.

Karnland O, Birgersson M. 2006. Montmorillonite stability. With special respect to KBS-3 conditions. SKB TR-06-11, Swedish Nuclear Fuel and Waste Management Co., Stockholm, Sweden.

Karnland O, Muurinen A, Karlsson F. 2005. Bentonite swelling pressure in NaCl solutions – experimentally determined data and model calculations. In: Advances in understanding engineered clay barriers (EE. Alonso and A. Ledesma, eds.). Taylor and Frances Group, London.

Komine H, Ogata N. 1994. Experimental study on swelling characteristics of compacted bentonite. Canadian Geotechnical Journal, 31 (4), 478–490.

Komine H, Ogata N. 1996. Prediction for swelling characteristics of compacted bentonite. Canadian Geotechnical Journal, 33 (1), 11–22.

Laird DA. 1996. Model for crystalline swelling of 2:1 phyllosilicates. Clays and Clay Minerals, 44 (4), 553–559.

Leroy P, Revil A, Altmann S, Tournassat, C. 2007. Modeling the composition of the pore water in a clay-rock geological formation (Callovo-Oxfordian, France). Geochimica Cosmochimica Acta, 71, 1087–1097.

Low PF. 1979. The swelling of clay. I: Basic concepts and empirical equations. Soil Science Society of America Journal, 43, 473–484.

Low PF. 1980. The swelling of clay. II: Montmorillonites. Soil Science Society of America Journal, 44, 667–676.

Low PF. 1987. Structural component of the swelling pressure of clays. Langmuir, 3, 18.

Kruyt HR. (ed.). 1952. Colloid science. Elsevier, New York.

Marshall CE. 1948. Theory of selective membrane behavior. Journal of Physical Chemistry, 52, 1284–1295.

Madsen FT, Müller-VonMoos M. 1989. The swelling behaviour of clays. Applied Clay Science, 4, 143-156.

Muurinen A. 2006. Ion concentration caused by an external solution into the porewater of compacted bentonite. Working Report 2006-96, Posiva Oy, Olkiluoto, Finland.

Muurinen A, Karnland O, Lehikoinen J. 2004. Ion concentration caused by an external solution into the porewater of compacted bentonite. Physics and Chemistry of the Earth, 29, 119–127.

Pastina B, Hellä P. 2006. Expected evolution of a spent nuclear fuel repository at Olkiluoto. Posiva 2006-05, Posiva Oy, Olkiluoto, Finland.

Pokrovskii VA, Helgeson HC. 1995. Thermodynamic properties of aqueous species and the solubilities of minerals at high pressures and temperatures: The system $Al_2O_3$-$H_2O$-NaCl. American Journal of Science, 295, 1255–1342.

Posiva 2010. TKS-2009. Nuclear waste management at Olkiluoto and Loviisa power plants. Posiva, Oy, Olkiluoto, Finland.

Savage D. 2005. The effects of high salinity groundwater on the performance of clay barriers. SKI Report 2005:54, Swedish Nuclear Power Inspectorate, Stockholm, Sweden.

SKB 2006a. Long-term safety for KBS-3 repositories at Forsmark and Laxemar – a first evaluation: Main report of the SR-Can project. SKB TR-06-09, Swedish Nuclear Fuel and Waste Management Co., Stockholm, Sweden.

SKB 2006b. Buffer and backfill process report for the safety assessment SR-Can. SKB TR-06-18, Swedish Nuclear Fuel and Waste Management Co., Stockholm, Sweden.

Skipper NT, Lock PA, Titiloye JO, Swenson J, Mirza ZA, Howells WS, Fernandez-Alonso F. 2006. The structure and dynamics of 2-dimensional fluids in swelling clays. Chemical Geology, 230, 182–196.

Sridharan A. 1997. Prediction of swelling characteristics of compacted bentonite: Discussion. Canadian Geotechnical Journal, 34, 1004.

Yong RN, Mohamed AMO, Warkentin BP. 1992. Principles of contaminant transport in soils. Development in Geotechnical Engineering, 73, Elsevier Publ. Co., Amsterdam.